© 2017. Published by The Company of Biologists Ltd | Development (2017) 144, 1851-1862 doi:10.1242/dev.146175

RESEARCH ARTICLE

Sec71 functions as a GEF for the small GTPase Arf1 to govern dendrite pruning of *Drosophila* sensory neurons

Yan Wang[1,2], Heng Zhang[1], Meng Shi[3], Yih-Cherng Liou[1,2], Lei Lu[3] and Fengwei Yu[1,2,4,*]

ABSTRACT

Pruning, whereby neurons eliminate their excess neurites, is central for the maturation of the nervous system. In *Drosophila*, sensory neurons, ddaCs, selectively prune their larval dendrites without affecting their axons during metamorphosis. However, it is unknown whether the secretory pathway plays a role in dendrite pruning. Here, we show that the small GTPase Arf1, an important regulator of the secretory pathway, is specifically required for dendrite pruning of ddaC/D/E sensory neurons but dispensable for apoptosis of ddaF neurons. Analyses of the GTP- and GDP-locked forms of Arf1 indicate that the cycling of Arf1 between GDP-bound and GTP-bound forms is essential for dendrite pruning. We further identified Sec71 as a guanine nucleotide exchange factor for Arf1 that preferentially interacts with its GDP-bound form. Like Arf1, Sec71 is also important for dendrite pruning, but not for apoptosis, of sensory neurons. Arf1 and Sec71 are interdependent for their localizations on Golgi. Finally, we show that the Sec71/Arf1-mediated trafficking process is a prerequisite for Rab5-dependent endocytosis to facilitate endocytosis and degradation of the cell-adhesion molecule Neuroglian (Nrg).

KEY WORDS: Pruning, Dendrite, Sensory neuron, Metamorphosis, Secretory pathway, *Drosophila*

INTRODUCTION

In the developing nervous systems, neurons often extend excessive neurites and form superfluous connections at early stages. Subsequent removal of those exuberant or inappropriate neurites without causing the death of parental neurons, a process known as pruning, is crucial for the refinement of neural circuits at late developmental stages (Luo and O'Leary, 2005; Riccomagno and Kolodkin, 2015; Schuldiner and Yaron, 2015). Neuronal pruning is a conserved process widely occurring in both vertebrates and invertebrates. In vertebrates, many neurons in the neocortex, neuromuscular system and hippocampal dentate gyrus prune their unwanted neurites to control the proper wiring of the nervous systems (Bagri et al., 2003; O'Leary and Koester, 1993; Tapia et al., 2012). In invertebrates, such as *Drosophila*, the nervous systems undergo drastic remodeling during metamorphosis, a transition stage from a larva to an adult fly (Kanamori et al., 2015a; Truman, 1990; Yu and Schuldiner, 2014). In the central nervous system (CNS), mushroom body (MB) γ neurons prune their dorsal and medial axon branches as well as entire dendrites (Lee et al., 1999). In the peripheral nervous system (PNS), some dorsal dendritic arborization (da) neurons, ddaC, ddaD and ddaE, selectively eliminate their larval dendrites without affecting their axons (Kuo et al., 2005; Williams and Truman, 2005), whereas ddaF neurons are apoptotic during early metamorphosis (Williams and Truman, 2005). The pruning event involves both local degeneration and retraction (Luo and O'Leary, 2005), resembling neurodegeneration associated with brain injury and neurodegenerative diseases. Thus, a complete understanding of cellular and molecular mechanisms of developmental pruning would shed some light on pathological neurodegeneration following neurological diseases and injury.

In *Drosophila*, ddaC sensory neurons have emerged as an attractive model system with which to elucidate the molecular and cellular mechanisms of dendrite-specific pruning during early metamorphosis. In response to the steroid-molting hormone 20-hydroxyecdysone (ecdysone) at the late larval stage, ddaC neurons sever the proximal region of their dendrites and subsequently undergo rapid fragmentation of the severed dendrites, as well as dendritic clearance via phagocytosis (Fig. 1A) (Kuo et al., 2005; Williams and Truman, 2005). It has been well documented that the Ecdysone Receptor and its co-receptor Ultraspiracle are required to activate the expression of several downstream targets to initiate dendrite pruning (Yu and Schuldiner, 2014). We and others have recently reported the identification of endocytic pathways that are crucial for dendrite pruning (Kanamori et al., 2015b; Zhang et al., 2014). Rab5/Avalanche and ESCRT complexes, the components of the endocytic pathways, are required for downregulation of the L1-type cell adhesion molecule (L1-CAM) Neuroglian (Nrg) (Zhang et al., 2014). Nrg is drastically redistributed to endosomes and its protein levels are strongly downregulated prior to pruning, suggesting that massive Nrg endocytosis promotes dendrite pruning (Zhang et al., 2014). It is conceivable that Nrg endocytosis might be triggered by secreted ligands/signals through the secretory pathway. However, it is completely unknown whether the secretory pathway, an opposite route of the endocytic pathway, also plays a role in dendrite pruning of ddaC neurons.

The primary sites of the secretory pathway consist of the endoplasmic reticulum (ER), the Golgi apparatus and the *trans*-Golgi network in eukaryotic cells (Lippincott-Schwartz et al., 2000). Newly synthesized membrane proteins and lipids exit from the ER, pass through the Golgi complexes and are delivered to the plasma membrane via the post-Golgi exocytosis (Pfenninger, 2009). In developing neurons, the continuous addition of membrane proteins and lipids via the secretory pathway plays a key role in the outgrowth and elongation of dendrites and axons (Horton and Ehlers, 2004). Disruption of the ER-to-Golgi transport leads to the inhibition of dendritic or axonal growth in *Drosophila*

[1]Temasek Life Sciences Laboratory and Department of Biological Sciences, 1 Research Link, National University of Singapore, Singapore 117604. [2]NUS Graduate School for Integrative Sciences and Engineering, Centre for Life Sciences, Singapore 117456. [3]School of Biological Sciences, Nanyang Technological University, 60 Nanyang Drive, Singapore 637551. [4]Neuroscience and Behavioral Disorder Program, Duke-NUS Graduate Medical School Singapore, 8 College Road, Singapore 169857.

*Author for correspondence (fengwei@tll.org.sg)

F.Y., 0000-0003-0268-199X

Received 28 October 2016; Accepted 29 March 2017

Development (2017) 144, 1851-1862 doi:10.1242/dev.146175

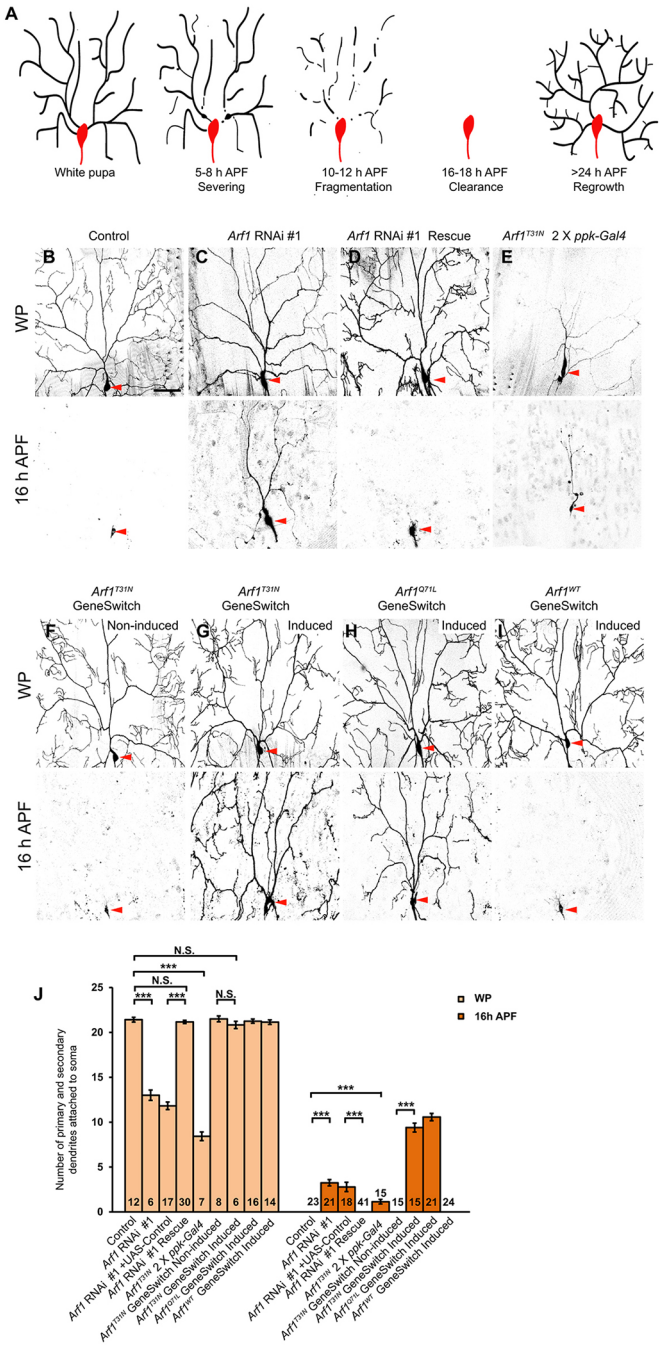

Fig. 1. Arf1 GTPase is crucial for dendrite pruning in ddaC sensory neurons. (A) A schematic representation of dendrite pruning in ddaC neurons during early metamorphosis. (B-I) Dendrites of control RNAi (B), *Arf1* RNAi #1 (C), *Arf1* RNAi #1 rescue (D), $Arf1^{T31N}$ (E), *GeneSwitch-Gal4-2295*-driven $Arf1^{T31N}$ (F, non-induced; G, induced), $Arf1^{Q71L}$ (H) and $Arf1^{WT}$ (I) ddaC neurons at WP and 16 h APF stages. Red arrowheads indicate the ddaC somas. (J) Quantification of the average number of primary and secondary ddaC dendrites. Scale bar: 50 µm. Error bars represent s.e.m. N.S., not significant; ***P<0.001, as assessed by one-way ANOVA and Bonferroni test.

sensory neurons and rodent hippocampal neurons (Aridor and Fish, 2009; Ye et al., 2007). In an attempt to isolate novel players of dendrite pruning, we carried out a large-scale RNA interference (RNAi) screen and identified ADP-ribosylation factor 1(Arf1), also known as ADP-ribosylation factor at 79F (Arf79F), as an important player for dendrite pruning in ddaC sensory neurons. Arf1 is a small GTPase and belongs to the Class I Arf family (D'Souza-Schorey and Chavrier, 2006; Gillingham and Munro, 2007). It has been reported that Arf1 can recruit COPI coat proteins on *cis*-Golgi and clathrin adaptor proteins, such as AP-1, AP-3 and GGAs, on *trans*-Golgi in a GTP-dependent manner, thereby facilitating vesicle formation and trafficking (Cherfils, 2014). Studies from yeast and mammals indicate that Arf1 is activated by two conserved families of guanine nucleotide exchange factors (GEFs), including the Gea1/GBF1 family on *cis*-Golgi and the Sec7/BIG family on *trans*-Golgi (Gillingham and Munro, 2007). Arf1 cycles between GDP- and GTP-bound forms, and both the GTP- and GDP-locked forms can interfere with its functions and disrupt secretory trafficking (Dascher and Balch, 1994). In mammalian hippocampal neurons, overexpression of the GTP-locked form of Arf1 ($Arf1^{Q71L}$), which abolishes Arf1 activity, inhibits dendrite growth (Horton et al., 2005). The mammalian Arf1GEF, BIG2, is required for vesicle trafficking and mutations in human *BIG2* (*ARFGEF2* – HGNC) lead to autosomal recessive periventricular heterotopia with microcephaly (ARPHM), a brain disorder characterized by defective neural proliferation and migration (Ferland et al., 2009; Sheen et al., 2004). Thus, various studies have documented that the secretory pathway plays a crucial role in neurite growth and extension in developing neurons. However, very little is known about its role in regulating neurite pruning, a developmental degenerative process.

Here, we report the identification of Arf1 as an important player of dendrite pruning in ddaC sensory neurons. The cycling of Arf1 between GDP-bound and GTP-bound forms is essential for dendrite pruning. We also further identify Sec71 as a GEF for Arf1 in *Drosophila*. We show that Sec71, like Arf1, is cell-autonomously required for dendrite pruning of ddaC/D/E sensory neurons but not for apoptosis of ddaF neurons during early metamorphosis. Arf1 and Sec71 colocalize on Golgi apparatus and regulate secretory vesicle biogenesis in ddaC neurons. Furthermore, we show that Sec71/Arf1-dependent secretory pathway acts upstream of Rab5-dependent endocytosis and facilitates the internalization and downregulation of the cell-adhesion molecule Nrg prior to dendrite pruning. Thus, our study demonstrates a novel and important role of Arf1/Sec71-mediated secretory pathway in promoting developmental pruning via the regulation of Nrg endocytosis.

RESULTS

Arf1 GTPase is crucial for dendrite pruning but not for neuronal apoptosis

To identify novel players of dendrite pruning in ddaC sensory neurons, we conducted a genome-wide RNAi screen by crossing the class IV da neuron driver *ppk-Gal4* (Grueber et al., 2003) and *UAS-Dicer2* with a large collection of RNAi lines from Vienna and Bloomington *Drosophila* stock centers (Kirilly et al., 2009). From this screen, we isolated two distinct RNAi lines, v23082 (#1) and v103572 (#2), corresponding to *Arf1*. In *Drosophila*, Arf1 was reported to regulate planar cell polarity, blood cell homeostasis and lamellipodium formation (Carvajal-Gonzalez et al., 2015; Humphreys et al., 2012; Khadilkar et al., 2014). The expression of these *Arf1* RNAi transgenes, via *ppk-Gal4*, led to consistent dendrite pruning defects in the vast majority of ddaC neurons at 16 h after puparium formation (APF) (90% and 100%, respectively; Fig. 1C; Fig. S1A). On average, 3.2 primary and secondary dendrites remained attached to *Arf1* RNAi ddaC neurons at 16 h APF (Fig. 1J). Those larval dendrites were eventually pruned away at 32 h APF (Fig. S1D). By contrast, all larval dendrites were completely eliminated in the control neurons expressing an irrelevant RNAi line at 16 h APF

Development (2017) 144, 1851-1862 doi:10.1242/dev.146175

(Fig. 1B). Development of larval dendrite arbors was also impaired in *Arf1* RNAi ddaC neurons, as the numbers of primary and secondary dendrites at the white prepupal (WP) stage were reduced; moreover, elaboration of high-order dendrites was also severely affected (Fig. 1C,J). To validate the RNAi knockdown phenotypes, we generated a synthetic RNAi-resistant transgene that bears minimal homology to the *Arf1* dsRNA sequence (#1) but encodes the wild-type Arf1 protein. Both dendrite pruning and morphology defects observed in *Arf1* RNAi (#1) ddaC neurons were fully rescued by co-expression of this RNAi-resistant *Arf1* transgene (Fig. 1D,J), confirming the specificity of the *Arf1* RNAi effect.

Arf1 is a small GTPase that is required for secretory membrane biogenesis and transport (D'Souza-Schorey and Chavrier, 2006). It can cycle between an inactive GDP-bound form and an active GTP-bound form (Gillingham and Munro, 2007). We expressed $Arf1^{T31N}$, a GDP-locked form of Arf1, in ddaC neurons. Consistently, the expression of $Arf1^{T31N}$, via two copies of *ppk-Gal4* driver, also resulted in a dendrite pruning defect at 16 h APF (Fig. 1E,J). The mild pruning defect is probably due to an initial dendrite development defect, as few WP dendrites were present in the vicinity of $Arf1^{T31N}$ ddaC neurons (Fig. 1E,J). The cytological location of the *Arf1* gene near the centromere precludes our MARCM clonal analysis. To circumvent the requirement of Arf1 for initial dendrite development, we induced $Arf1^{T31N}$ expression at the middle third instar larval stage (90-96 h after egg laying, AEL) using the gene-switch system. Full penetrance of dendrite pruning defect was observed in the $Arf1^{T31N}$-expressing ddaC neurons derived from animals fed with RU486 for 6 h (100%; Fig. 1G), in contrast to no pruning defect observed in non-fed animals (Fig. 1F). Approximately 9.4 primary and secondary dendrites persisted with the attachment to the soma of $Arf1^{T31N}$-induced ddaC neurons at 16 h APF (Fig. 1J), indicating a severe dendrite pruning defect. Moreover, pulse expression of $Arf1^{T31N}$ did not impair initial ddaC dendritic development and morphology, as shown at the WP stage (Fig. 1G,J). These data highlight that the $Arf1^{T31N}$-associated dendrite pruning defect is not a secondary consequence of its initial dendrite arborization defect. Thus, Arf1 is required to promote dendrite pruning in ddaC sensory neurons.

Both the GTP- and GDP-locked forms of Arf1 can interfere with its functions in the secretory pathway (Dascher and Balch, 1994). Indeed, like that of $Arf1^{T31N}$, pulse expression of $Arf1^{Q71L}$, a GTP-locked form of Arf1, also led to strong dendrite severing defects, with the persistence of 10.6 primary and secondary dendrites at 16 h APF in RU486-fed animals (100%, Fig. 1H). However, no obvious pruning defect phenotype was observed in ddaC neurons expressing wild-type Arf1 protein ($Arf1^{WT}$) at 16 h APF with two copies of the continuously expressing driver *ppk-Gal4* (Fig. S1A) or the gene-switch system (Fig. 1I,J). These results strongly support the notion that the cycling of Arf1 between GDP-bound and GTP-bound forms is essential for normal progression of dendrite pruning. In addition to ddaC neurons, ddaD/E sensory neurons also completely eliminated their dendrites by 19 h APF (Fig. S1B). $Arf1^{T31N}$-expressing mutant ddaD/E neurons retained some of their larval dendrites attached to their soma (83%, Fig. S1B). Wild-type ddaF neurons are apoptotic during early metamorphosis (Williams and Truman, 2005). Interestingly, ddaF neurons expressing $Arf1^{T31N}$ or *Arf1* RNAi constructs were eliminated (Fig. S1B), similar to wild-type ddaF neurons, suggesting that Arf1 is dispensable for ddaF apoptosis. Collectively, Arf1 plays an important role in regulating dendrite pruning, rather than apoptosis, of sensory neurons; the cycling of GDP-Arf1 and GTP-Arf1 is essential for normal dendrite pruning.

Arf1 is localized on the Golgi compartments in ddaC sensory neurons

To assess subcellular localization of Arf1 in *Drosophila*, we generated an antibody against Arf1 and performed the immunostaining with the anti-Arf1 antibody in ddaC sensory neurons. The anti-Arf1 antibody is specific, as its signals were completely eliminated by both *Arf1* RNAi knockdowns (Fig. S2A). We observed many Arf1-positive punctate structures in wild-type ddaC soma and these discrete puncta were colocalized with galactosyltransferase-GFP (GalT-GFP), a *trans*-Golgi marker (Fig. 2A). Arf1 punctate structures were partially colocalized and juxtaposed with the *cis*-Golgi marker GM130 (Fig. 2B). Likewise, Arf1 was also colocalized with another Golgi protein: Lava Lamp (Lva) (Fig. S2B). Arf1-positive puncta were also localized next to the ER exit site marker Sec31-mCherry (Fig. 2C). However, Arf1 did not overlap with the recycling endosomal marker Rab4-mRFP, the early endosomal marker GFP-Rab5 and the mitochondrial marker Mito-GFP (Fig. S2C-E).

We then determined whether Arf1 regulates the integrity of the Golgi apparatus in ddaC neurons. We observed that GalT-GFP punctate structures were completely disrupted, as GalT-GFP signals became diffused in the soma of either $Arf1^{T31N}$ gene-switch (Fig. 2D) or *Arf1* RNAi (Fig. S2F) mutant ddaC neurons, compared with those bright puncta in wild type (Fig. 2A′). Similarly, GalT-GFP-positive (Fig. S2H) or ManII-VENUS (Fig. 2H′) signals were also diffused in the dendrites of *Arf1 RNAi* ddaC neurons, compared with the controls (Fig. S2G, Fig. 2G′, respectively). The GM130 marker was also strongly reduced in size and number in $Arf1^{T31N}$ neurons (Fig. 2E). These data indicate that the integrity of Golgi apparatus is disrupted in *Arf1* mutant neurons. By contrast, the Sec31-mCherry marker was still distributed as many discrete punctate structures, although the numbers of their respective puncta were slightly reduced (Fig. 2F). These data indicate that Arf1 regulates the integrity of the Golgi apparatus. Thus, Arf1 is predominantly localized on the Golgi compartments and is important for the integrity of the Golgi structures in ddaC neurons.

Sec71, a Sec7 domain-containing protein, is required for the regulation of dendrite pruning, rather than apoptosis, in sensory neurons

We then took advantage of RNAi and biochemical approaches to identify an important Arf1GEF that is also involved in dendrite pruning. Arf1 can be activated from a GDP-bound state to GTP-bound state by Sec7 domain-containing GEFs (Gillingham and Munro, 2007). We first examined the potential requirements of six Sec7 domain-containing GEFs from the *Drosophila* genome using RNAi. Among them, we isolated two independent RNAi transgenes, BL32366 (#1) and v100300 (#2), which both target *Sec71*. Sec71 is a GEF with a catalytic Sec7 domain, which is more closely related to the BIG1/BIG2 family (Christis and Munro, 2012). Mutations in *BIG2*, a human counterpart of *Sec71*, lead to defective vesicle trafficking, impaired cell adhesion and ARPHM disease (Sheen et al., 2004). Notably, RNAi-mediated knockdown of *Sec71* led to complete penetrance of dendrite pruning defects in all ddaC neurons with 5.7 and 4.7 primary and secondary dendrites attached to their soma at 16 h APF (Fig. 3B,D,G). Those larval dendrites were eventually pruned away at 32 h APF (Fig. S1D). By contrast, all larval dendrites were completely pruned in the control neurons expressing an irrelevant RNAi line at 16 h APF (Fig. 3A,G). Similar to *Arf1* mutants, *Sec71* RNAi ddaC neurons exhibited simplified dendrite arbors at larval and WP stages (WP: Fig. 3B,D,G; wL3: Fig. S3E). Co-expression of an RNAi-resistant

Development (2017) 144, 1851-1862 doi:10.1242/dev.146175

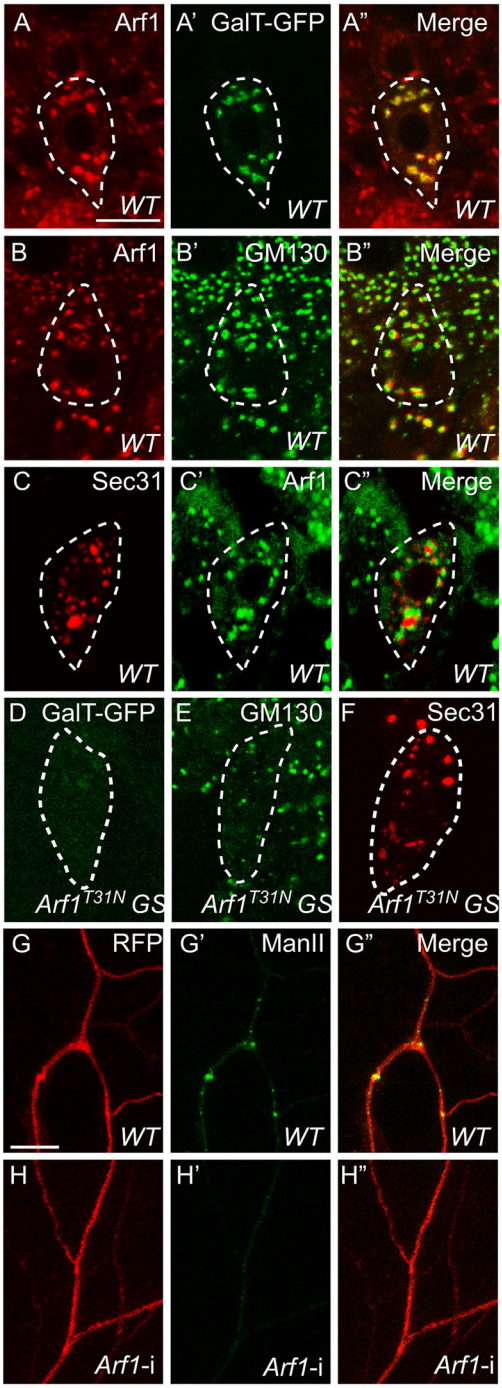

Fig. 2. Arf1 is localized on the Golgi compartments in ddaC sensory neurons. (A-A″) Distribution of Arf1 and *trans*-Golgi marker GalT-GFP in wild-type (WT) ddaC neurons expressing a *UAS-GalT-GFP* transgene. (B-B″) Distribution of Arf1 and *cis*-Golgi marker GM130 in wild-type ddaC neurons. (C-C″) Distribution of Arf1 and ER exit point marker Sec31-mCherry in wild-type ddaC neurons expressing a *UAS-Sec31-mCherry* transgene. (D-F) Distribution of GalT-GFP (D), GM130 (E) and Sec31-mCherry (F) in $Arf1^{T31N}$-expressing ddaC neurons. (G-H″) ManII-Venus-positive dendritic Golgi outpost in wild-type (G-G″) and *Arf1* RNAi (H-H″). GS denotes gene switch. Scale bars: 10 µm. ddaC somas are indicated by dashed lines.

Sec71 transgene fully rescued both dendrite pruning and morphology defects associated with *Sec71* RNAi (#1) ddaC neurons (Fig. 3C,G), confirming that the RNAi transgene specifically targets *Sec71*.

Sec7 domain-containing ArfGEFs activate Arf proteins from the GDP-bound state to the GTP-bound state. The glutamic acid-to-lysine substitution in the conserved Sec7 domain behaves as a catalytically inactive form, as shown for the corresponding mutation in the human ArfGEF GBF1 (E794K) (Garcia-Mata et al., 2003). As described below, the E794K change indeed abolished the GEF activity of the Sec71 protein in a GEF assay (Fig. 4E,F), thus behaving as a dominant-negative form (hereafter referred to as $Sec71^{DN}$). To determine a specific requirement of *Sec71* function for dendrite pruning, we used the gene-switch system to pulse induce the expression of $Sec71^{DN}$ at the middle third instar larval (90-96 h AEL) stage, which did not affect initial dendrite development and morphology in ddaC neurons at the WP stage (Fig. 3F). Strong dendrite severing defects were observed in all $Sec71^{DN}$-expressing ddaC neurons derived from RU486-induced animals and an average of 9.7 primary and secondary dendrites remained unpruned at 16 h APF (Fig. 3F,G), in contrast to no larval dendrites being present in non-induced animals (Fig. 3E,G). Some larval dendrites in $Sec71^{DN}$-expressing ddaC neurons remained attached by 24 h APF (data not shown). Continuous expression of $Sec71^{DN}$ via *ppk-Gal4* also caused simplified dendrite arbors in ddaC neurons (data not shown). Thus, the gene-switch experiments strongly suggest that the $Sec71^{DN}$ dendrite pruning defect is not a secondary effect of its initial dendrite arborization defect. Thus, Sec71 regulates dendrite pruning of ddaC neurons, which is separable from its role in initial dendrite growth.

To further verify the functions of Sec71 in dendrite pruning, we generated a strong mutant allele, $Sec71^{EX11}$, from the mobilization of the P-element insertion $Sec71^{GS16990}$ (Fig. S3A). MARCM clones of $Sec71^{EX11}$ consistently exhibited simple dendrite arbors and dendrite pruning defects (Fig. S3B). Reintroduction of the Sec71 protein into $Sec71^{EX11}$ mutant ddaC neurons fully restored the complex dendrite arbors and rescued the pruning defects (Fig. S3B). In addition to ddaC neurons, ddaD/E neurons expressing $Sec71^{DN}$ also exhibited dendrite pruning defects, as their larval dendrites were attached to their soma by 19 h APF (50%, Fig. S3C). $Sec71^{DN}$-expressing ddaF neurons were eliminated by 16 h APF (Fig. S3C), similar to wild-type neurons. Other known ArfGEFs, namely Steppke and Arf6GEF [encoded by the *loner* (*siz* – FlyBase) gene], are dispensable for ddaC dendrite pruning (Fig. S3D).

Sec71 is an Arf1GEF that preferentially interacts with GDP-bound Arf1

To examine the possibility that Sec71 functions as an Arf1GEF, we first determined the physical interaction between Arf1 and Sec71. We overexpressed the full-length Sec71 protein in S2 cells and performed GST pull-down experiments using various GST fusion proteins containing wild-type Arf1 ($Arf1^{WT}$), a GTP-bound form ($Arf1^{Q71L}$) or a GDP-bound form ($Arf1^{T31N}$). GEF proteins preferentially bind to the nucleotide-free form or the GDP-bound form, but not the GTP-bound form. Importantly, Sec71 possessed a strong binding affinity for $Arf1^{WT}$ and GDP-Arf1 but not for GTP-Arf1 (Fig. 4A). To confirm these interactions, we conducted co-immunoprecipitation experiments for Sec71 and Arf1. Similarly, we observed that Sec71 interacted strongly with $Arf1^{WT}$ and GDP-Arf1, but weakly with GTP-Arf1 (Fig. 4B). Moreover, the interaction between Sec71 and wild-type Arf1 was attenuated in the presence of excess γ-GTP, a non-hydrolyzable GTP analog (Fig. S4A). Thus, Sec71 preferentially interacts with the nucleotide-free form or the GDP-bound form of Arf1.

To further substantiate that Sec71 is an Arf1GEF, we investigated whether Sec71 is able to specifically catalyze the guanine

Development (2017) 144, 1851-1862 doi:10.1242/dev.146175

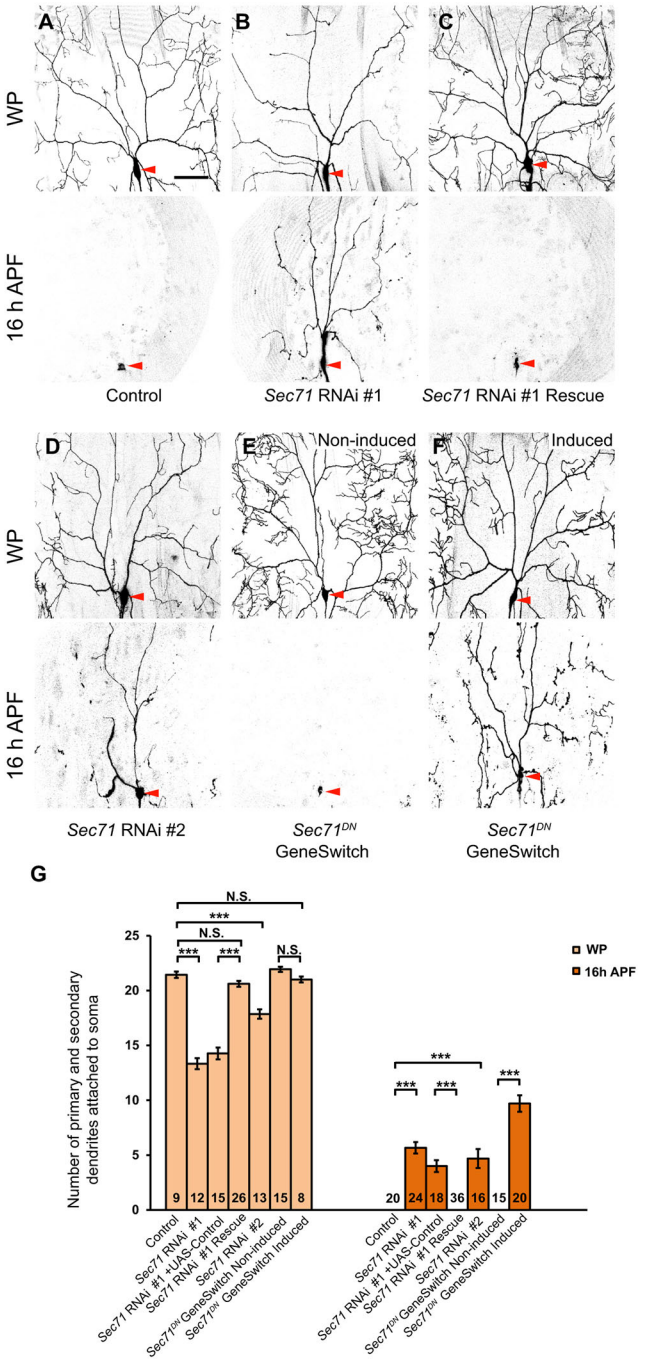

Fig. 3. Sec71 is crucial for the regulation of dendrite pruning in sensory neurons. (A-E) Dendrites of wild-type (A), *Sec71* RNAi #1 (B), Sec71 RNAi#1 rescue (C), Sec71 RNAi#2 (D) and *GeneSwitch-Gal4-2295*-driven $Sec71^{DN}$ (E, non-induced; F, induced) ddaC neurons at WP and 16 h APF stages. Red arrowheads indicate the ddaC somas. (G) Quantification of the average number of primary and secondary ddaC dendrites. Scale bar: 50 µm. Error bars represent s.e.m. N.S., not significant; ***P<0.001, as assessed by one-way ANOVA and Bonferroni test.

nucleotide exchange of Arf1. We monitored the quantum yield of a non-hydrolyzable and fluorescent analogue of GTP, which increases upon binding to GTPase. His-Arf1 was incubated with different GST proteins, and the levels of the guanine nucleotide exchange of Arf1 were measured via the increase of fluorescence intensity. Sec71 tagged with GST resulted in rapid kinetics of fluorescence increase (Fig. 4D), compared with the GST protein control (Fig. 4C). The inverse of time constant, 1/τ value, reflects the intrinsic exchange activity of an GEF. The exchange activity of GST-Sec71 on Arf1 was significantly higher than that of the GST control (Fig. 4F). This exchange activity was abolished by the catalytically incompetent form of Sec71 (GST-$Sec71^{EK}$) (Fig. 4E,F). As a control, we did not observe any exchange activity of GST-Sec71 on another small GTPase Arl1 (Fig. S4B). Thus, Sec71 possesses specific GEF activity toward Arf1.

We further provided genetic evidence to strengthen the notion that Arf1 functions downstream of Sec71 to regulate dendrite pruning. We had observed that the expression of $Arf1^{Q71L}$, like $Arf1^{T31N}$, caused a block of dendrite pruning, whereas the expression of wild-type Arf1 ($Arf1^{WT}$) did not (Fig. 1G,H,I). The GTP-locked form $Arf1^{Q71L}$ was unable to recue *sec71* RNAi knockdown in terms of its dendrite pruning defects (data not shown) because excess GTP-Arf1, induced by $Arf1^{QL}$, is not functional. We therefore overexpressed $Arf1^{WT}$ in *Sec71* RNAi ddaC neurons to investigate its potential rescue effect on dendrite pruning. Importantly, the expression of wild-type Arf1 in *Sec71* RNAi mutant ddaC (Fig. 4H,I) fully rescued the dendrite pruning defects, compared with the control UAS transgene (Fig. 4G,I). Moreover, overexpression of Arf1 also rescued the initial dendrite morphology defects at the WP stage (Fig. 4H,I). These data suggest that elevated level of Arf1 may enhance basal levels of activation/inactivation cycling, which is sufficient to override the requirement of the Arf1GEF Sec71 for dendrite pruning. As a control, the expression of another small GTPase $Arf6^{WT}$ was unable to suppress pruning defects in *Sec71* RNAi ddaC neurons (Fig. S4C). Collectively, Sec71 is an important GEF for Arf1 and facilitates the Arf1 cycling between GDP-bound and GTP-bound forms during dendrite pruning.

Sec71 is colocalized with Arf1 on Golgi and their localizations are interdependent

We next assessed the subcellular localization of Sec71 and its colocalization with Arf1. An antibody against the N-terminal epitope of Sec71 (see Fig. 6A) was generated and the specificity was confirmed in *Sec71* RNAi and $Sec71^{Ex11}$ mutant neurons (Fig. S5A). Using this anti-Sec71 antibody, we observed that endogenous Sec71 was distributed on punctate structures and colocalized with the *trans*-Golgi marker GalT-GFP (Fig. 5A-A″). The Sec71 signals were also colocalized with Arf1 (Fig. 5B-B″), partially with the *cis*-Golgi marker GM130 (Fig. 5C-C″) and adjacent to the ER exit marker Sec31-mCherry (Fig. 5D-D″). Likewise, Sec71 is also important for the integrity of the Golgi apparatus in ddaC neurons. In $Sec71^{DN}$ or *Sec71* RNAi-expressing ddaC neurons, the *trans*-Golgi marker GalT-GFP was completely diffused in their somas (Fig. 5E; Fig. S2F) compared with those in the wild type (Fig. 5A′). The *cis*-Golgi compartments, indicated by GM130 signals, were also strongly reduced in size and number in $Sec71^{DN}$-expressing ddaC neurons (Fig. 5F). The ER exit marker Sec31-mCherry remained largely similar in $Sec71^{DN}$-expressing ddaC neurons (Fig. 5G). These data suggest that the Golgi apparatus, particularly *trans*-Golgi, is severely disrupted in *Sec71* mutant neurons, similar to that in *Arf1* mutant neurons. Thus, *Sec71*, like Arf1, is localized on Golgi and is also required for the integrity of the Golgi compartment in ddaC neurons.

To determine the dependency of Arf1 and Sec71 localizations, we checked their endogenous proteins in either *Sec71* or *Arf1* mutants. In *Sec71* RNAi (Fig. 5H′) and $Sec71^{DN}$ gene-switch (Fig. 5H″) mutant ddaCs, Golgi localization of Arf1 was almost completely disrupted compared with wild-type neurons (Fig. 5H).

Development (2017) 144, 1851-1862 doi:10.1242/dev.146175

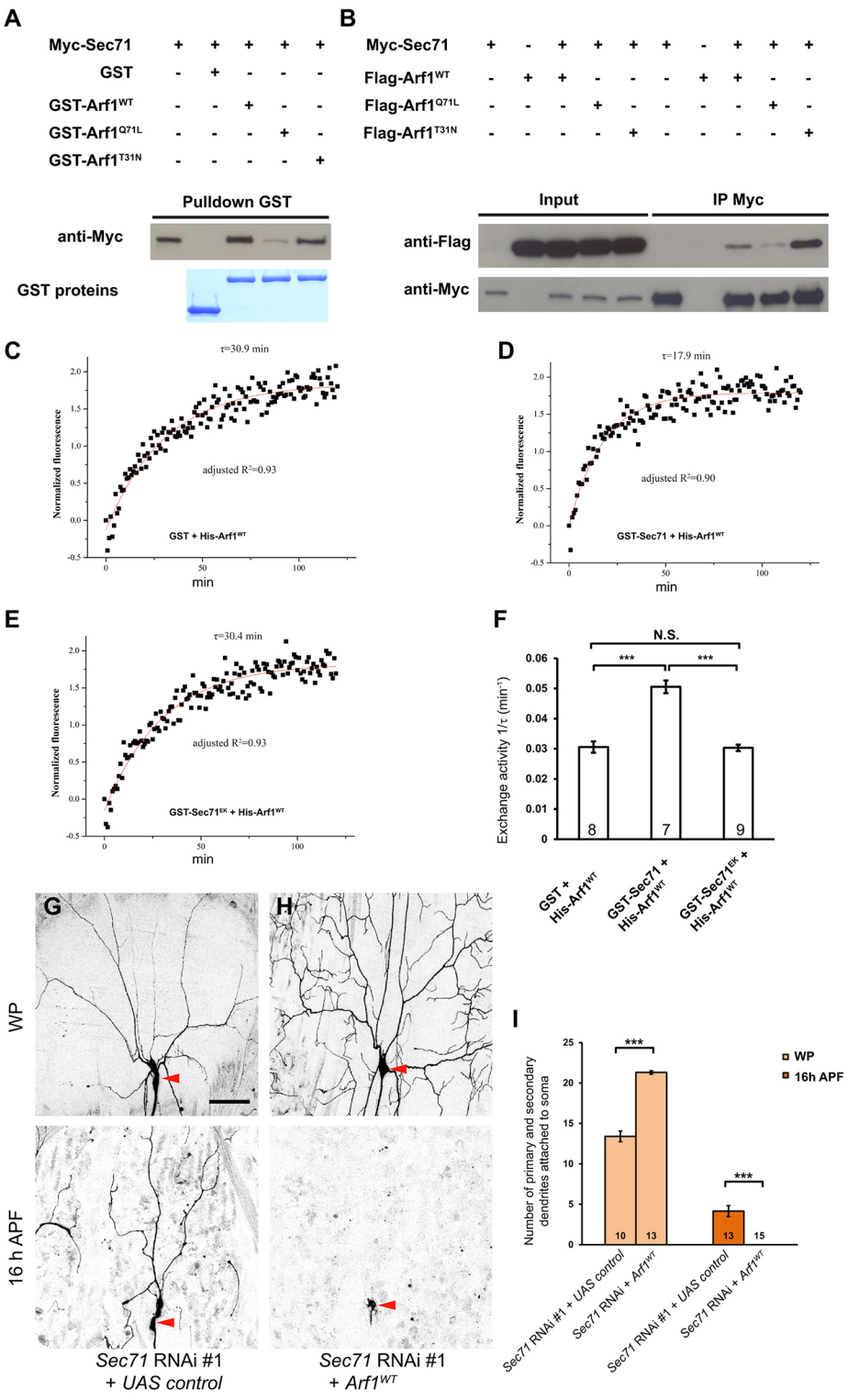

Fig. 4. Sec71 is an Arf1GEF that preferentially interacts with GDP-bound Arf1. (A) Sec71 associated strongly with Arf1^{WT} and Arf1^{T31N}, weakly with Arf1^{Q71L}, but not with GST alone in GST pull-down assays (n=3). Myc-Sec71 was transfected and expressed in S2 cells. (B) Sec71 associated strongly with Arf1^{WT} and Arf1^{T31N}, and weakly with Arf1^{Q71L} (n=3). S2 cells were co-transfected with Myc-Sec71 and different forms of Flag-Arf1. (C-E) Kinetics of the fluorescence increases of the GTP analog. Incubation with the GST-tagged Sec7 domain of Sec71 (Sec71) (D) led to more rapid kinetics towards Arf1, compared with the GST protein control (C) and GST-tagged mutated Sec7 domain (Sec71^{EK}) (E). (F) Quantification of the exchange activity reflected by the inverse of time constant, 1/τ value. (G,H) Dendrites of *Sec71* RNAi ddaC neurons co-expressing the UAS control (G) or Arf1^{WT} (H) at the WP stage and 16 h APF. Red arrowheads indicate the ddaC somas. (I) Quantification of the average number of primary and secondary ddaC dendrites. Scale bars: 50 µm. Error bars represent s.e.m. N.S., not significant; ***P<0.001, as assessed by one-way ANOVA and Bonferroni test.

Likewise, Sec71-positive puncta were largely absent in *Arf1* RNAi (Fig. 5I′) or *Arf1*^{T31N} gene-switch (Fig. 5I″) ddaC neurons compared with wild-type ddaC neurons (Fig. 5I). Occasionally, a couple of Sec71-labelled puncta were observed in *Arf1* RNAi ddaC (Fig. 5I′). Hence, Arf1 and Sec71 are mutually dependent on one another for their localizations on Golgi compartments. We therefore cannot exclude the possibility that their localization interdependence is due to the disruption of Golgi integrity caused by loss of either gene.

To investigate whether Arf1 and Sec71 regulate the formation of secretory vesicles in ddaC neurons, we made use of a GFP-tagged version of Sec15 (Sec15-GFP), a component of the exocyst complex, to monitor the distribution of secretory vesicles in sensory neurons. Sec15-GFP has been previously used to visualize a subset of secretory vesicles in neurons (Jafar-Nejad et al., 2005). In wild-type ddaC neurons, Sec15-GFP was distributed as discrete punctate structures in the somas (Fig. S5B), and was also enriched at dendritic branch points along major dendrites at the WP stage

Development (2017) 144, 1851-1862 doi:10.1242/dev.146175

(data not shown). Consistent with our observations, a previous study also reported Sec15 distribution in larval sensory neurons (Peng et al., 2015). Some Sec15-positive puncta were localized adjacent to or partially colocalized with the Arf1-positive Golgi apparatus (Fig. S5B). Notably, Sec15-GFP-positive puncta were completely absent in all *Arf1* RNAi (Fig. S5C) or *Sec71* RNAi (Fig. S5C) ddaC neurons. As a control, the ER exit marker Sec31-mCherry remained present in either $Arf1^{T31N}$ (Fig. 2F) or $Sec71^{DN}$ (Fig. 5G) mutant neurons. Thus, Arf1 and Sec71 appear to regulate biogenesis of secretory vesicles in ddaC sensory neurons.

To examine whether Arf1 and Sec71 regulate protein transport to the cell surface, we conducted a trafficking assay by detecting the levels of extracellular mCD8 epitope in a detergent-free condition. Via the gene-switch system, we pulse induced the expression of mCD8-GFP (murine CD8 fused to GFP) at the middle L3 stage and measured the levels of newly synthesized mCD8-GFP protein at the WP stage in ddaC neurons. In wild-type WP ddaC neurons, the extracellular mCD8 epitope was robustly detectable on the dendrites using the anti-mCD8 antibody in the absence of the detergent (Fig. S5D). We observed no or strongly reduced mCD8 signal on the surface of the dendrites in either $Arf1^{T31N}$ (Fig. S5D) or $Sec71^{DN}$ (Fig. S5D) ddaC neurons in the detergent-free condition. We found that overall GFP fluorescence representing both surface and internal pools of the protein in the soma of $Sec71^{DN}$ and $Arf1^{T31N}$ ddaC neurons was similar to that in wild-type neurons. In the trafficking assays, mCD8 signals were absent on the soma, axons and proximal regions of dendrites of ddaC neurons, presumably because these structures are tightly wrapped by glia and the antibody was not able to penetrate into the wrapped parts without the presence of detergent. Taken together, these observations show that Arf1 and Sec71 colocalize on Golgi and regulate protein secretion in sensory neurons.

The DCB domain of Sec71 is essential for its Golgi localization

Sec71 contains DCB (dimerization and cyclophilin binding) and HUS (homology upstream of Sec7) domains in its N-terminal region, a Sec7 domain in the middle region and HDS1-4 (homology downstream of Sec7) domains in its C-terminal region (Fig. 6A). We found that the Sec7 domain is essential for the Sec71 function in regulating dendrite pruning (Fig. 3F). To elucidate whether other domains of Sec71 are also required for its function, we generated a series of RNAi-resistant transgenes expressing various truncated proteins and examined their abilities to rescue *sec71* RNAi phenotypes (Fig. S6A). Although the expression of full-length Sec71 fully rescued the *Sec71* RNAi phenotypes in terms of dendrite arborization and pruning (Fig. 6C,G), the expression of DCB-deleted Sec71 protein was unable to significantly rescue the pruning defect in *sec71* RNAi ddaC neurons at 16 h APF (Fig. 6D,G) but partially restored the dendrite morphology (Fig. 6D,G). $Sec71^{\Delta DCB}$ did not appear to localize on Golgi (Fig. S6B), suggesting that the DCB domain of Sec71 is essential for its Golgi localization as well as for its function in regulating dendrite pruning. We observed that HDS2-4 domains are not important for Sec71 function, as the Sec71 variants deleting either HDS2-4 (Fig. 6E,G) or HDS3-4 domains (Fig. 6F,G), like the full-length protein, completely rescued both dendrite pruning and arborization defects. Apart from $Sec71^{\Delta DCB}$, all the other Sec71 variants were able to localize on Golgi (Fig. S6B). Thus, the DCB domain of Sec71 is important for proper function and Golgi localization of Sec71 during dendrite pruning.

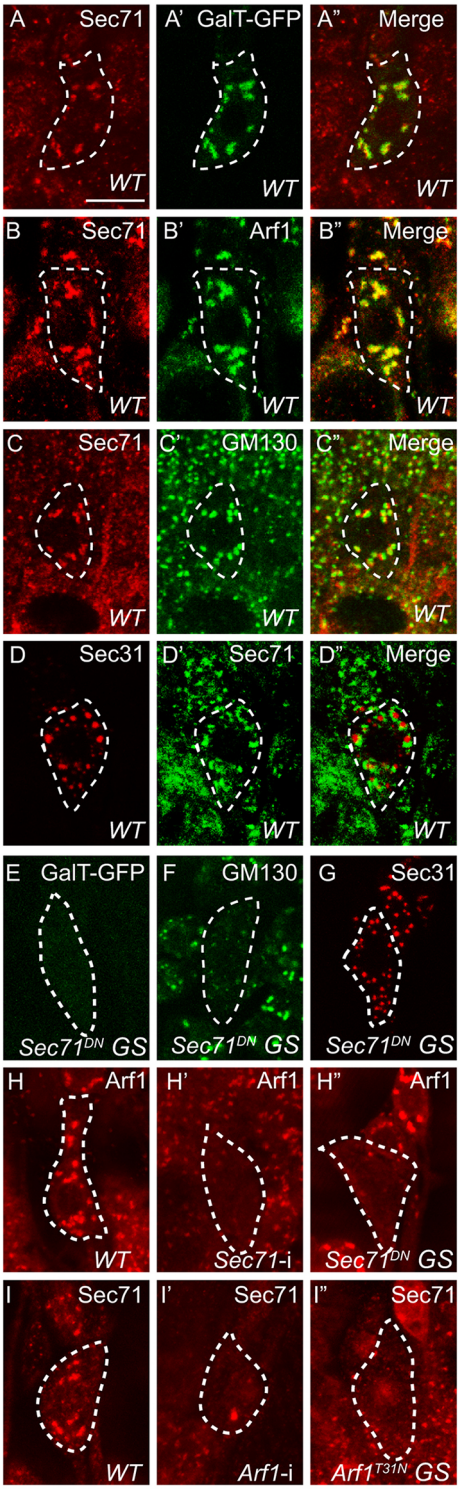

Fig. 5. Sec71 is colocalized with Arf1 on Golgi and their Golgi localizations are interdependent. (A-A″) Distribution of Sec71 and GalT-GFP in wild-type (WT) ddaC neurons expressing a *UAS-GalT-GFP* transgene. (B-B″) Distribution of Sec71 and Arf1 in wild-type ddaC neurons. (C-C″) Distribution of Sec71 and GM130 in wild-type ddaC neurons. (D-D″) Distribution of Sec71 and Sec31-mCherry in wild-type ddaC neurons expressing a *UAS-Sec31-mCherry* transgene. (E-G) Distribution of GalT-GFP (E), GM130 (F) and Sec31-mCherry (G) in $Sec71^{DN}$-expressing ddaC neurons. (H-H″) Distribution of Arf1 in wild-type (H), *Sec71* RNAi (H′) and $Sec71^{DN}$-expressing (H″) ddaC neurons. (I-I″) Distribution of Sec71 in wild-type (I), *Arf1* RNAi (I′) and $Arf1^{T31N}$-expressing (I″) ddaC neurons. GS denotes gene-switch. Scale bar: 10 µm. ddaC somas are marked by dashed lines.

Development (2017) 144, 1851-1862 doi:10.1242/dev.146175

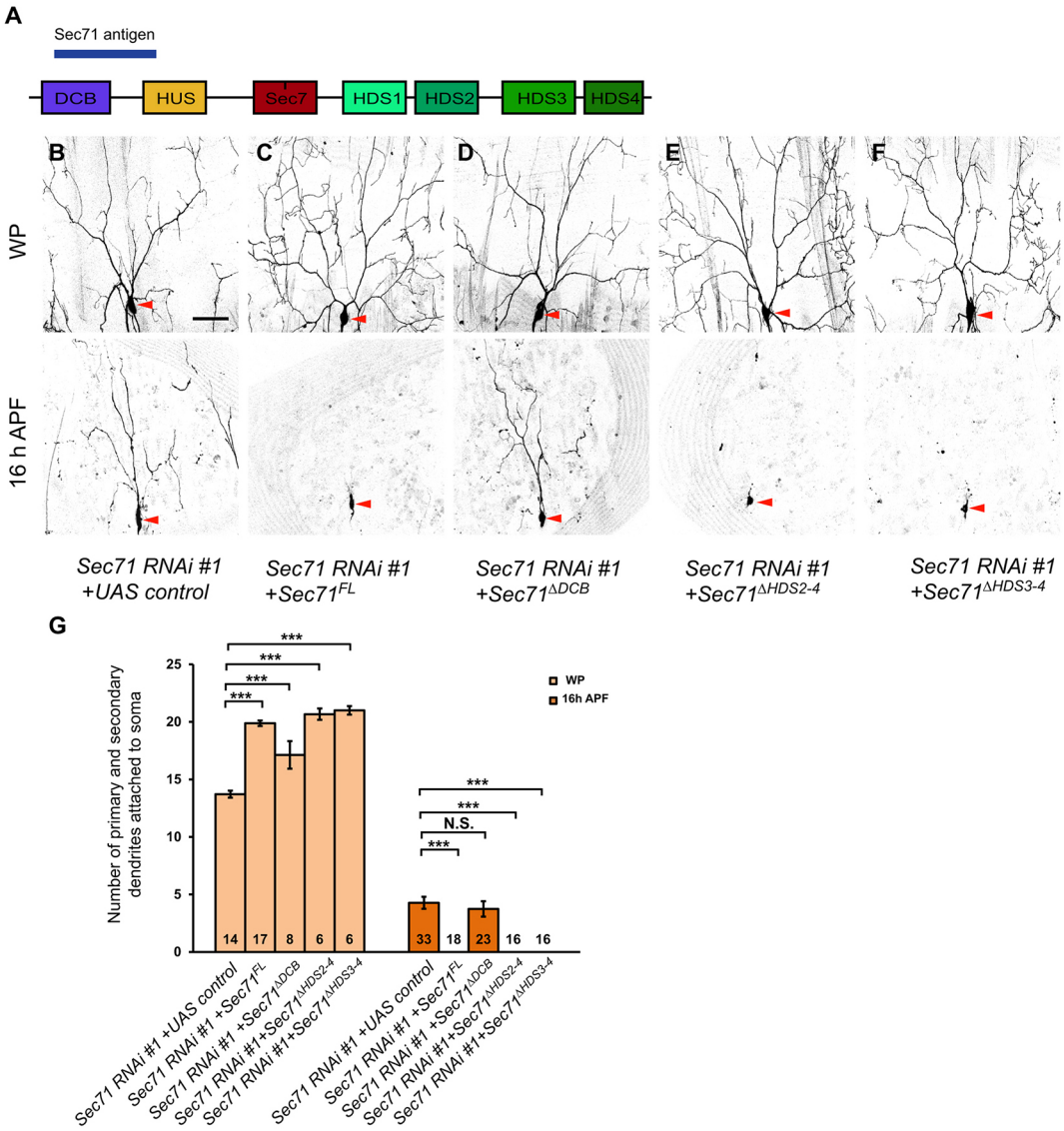

Fig. 6. Structure-function analysis of the Sec71 protein. (A) A schematic representation of the full-length Sec71 protein. (B-F) Dendrites of ddaC neurons co-expressing *Sec71* RNAi #1 and UAS control (B), *Sec71* RNAi #1 and full-length Sec71 (C), *Sec71* RNAi #1 and Sec71$^{\Delta DCB}$ (D), *Sec71* RNAi #1 and *Sec71$^{\Delta HDS2-4}$* (E), or *Sec71* RNAi #1 and *Sec71$^{\Delta HDS3-4}$* (F) at the WP stage and 16 h APF. Red arrowheads indicate the ddaC somas. (G) Quantification of the average number of primary and secondary ddaC dendrites. Scale bar: 50 µm. Error bars represent s.e.m. N.S., not significant; ***P<0.001, as assessed by one-way ANOVA and Bonferroni test.

Arf1/Sec71-mediated trafficking is a prerequisite for downregulation of the cell-adhesion molecule Nrg prior to dendrite pruning

We have previously reported that Rab5/ESCRT-dependent endocytic pathways downregulate the L1-CAM Nrg to promote dendrite pruning during early metamorphosis. In wild-type ddaC neurons, Nrg is drastically redistributed to early endosomes at 6 h APF prior to dendrite pruning and concomitantly its protein levels are also strongly reduced in the somas, dendrites and axons (Zhang et al., 2014). In *Rab5^{DN}* ddaC neurons, Nrg protein levels were significantly increased in the soma, dendrites and axons (Fig. 7B,E) (Zhang et al., 2014) compared with wild-type neurons (Fig. 7A,E). We therefore examined whether the Arf1/Sec71-dependent secretory pathway regulates the protein levels of Nrg at 6 h APF. Surprisingly, Nrg protein levels were significantly elevated in the dendrites, axons or soma of Arf1^{T31N} or Sec71^{DN} gene-switch ddaC neurons (Fig. 7C-E), similar to those in *Rab5^{DN}* neurons. Nrg protein levels in Arf1^{T31N} or Sec71^{DN} gene-switch ddaC neurons were comparable with those in Rab5^{DN}-expressing neurons (Fig. 7B-E). Moreover, Arf1 and Sec71 also regulate endosomal localization of Nrg prior to dendrite pruning. In wild-type neurons, Nrg protein mainly colocalized with the early endosomal marker GFP-2xFYVE at 6 h APF (Fig. S7A). By contrast, in Arf1^{T31N} or Sec71^{DN} gene-switch ddaC neurons, Nrg did not colocalize with those GFP-2xFYVE puncta (Fig. S7A), suggesting a block of Nrg endocytosis. Thus, Arf1 and Sec71, like Rab5, are required to facilitate Nrg endocytosis and downregulation prior to dendrite pruning.

To examine whether Arf1 and Sec71 regulate dendrite pruning upstream of Nrg function, we knocked down Nrg, via two independent *Nrg* RNAi transgenes, in *Arf1* RNAi- or *Sec71* RNAi-expressing ddaC neurons. Importantly, the expression of two independent *Nrg* RNAi transgenes, both of which efficiently knocked down Nrg protein (Zhang et al., 2014), dramatically

Development (2017) 144, 1851-1862 doi:10.1242/dev.146175

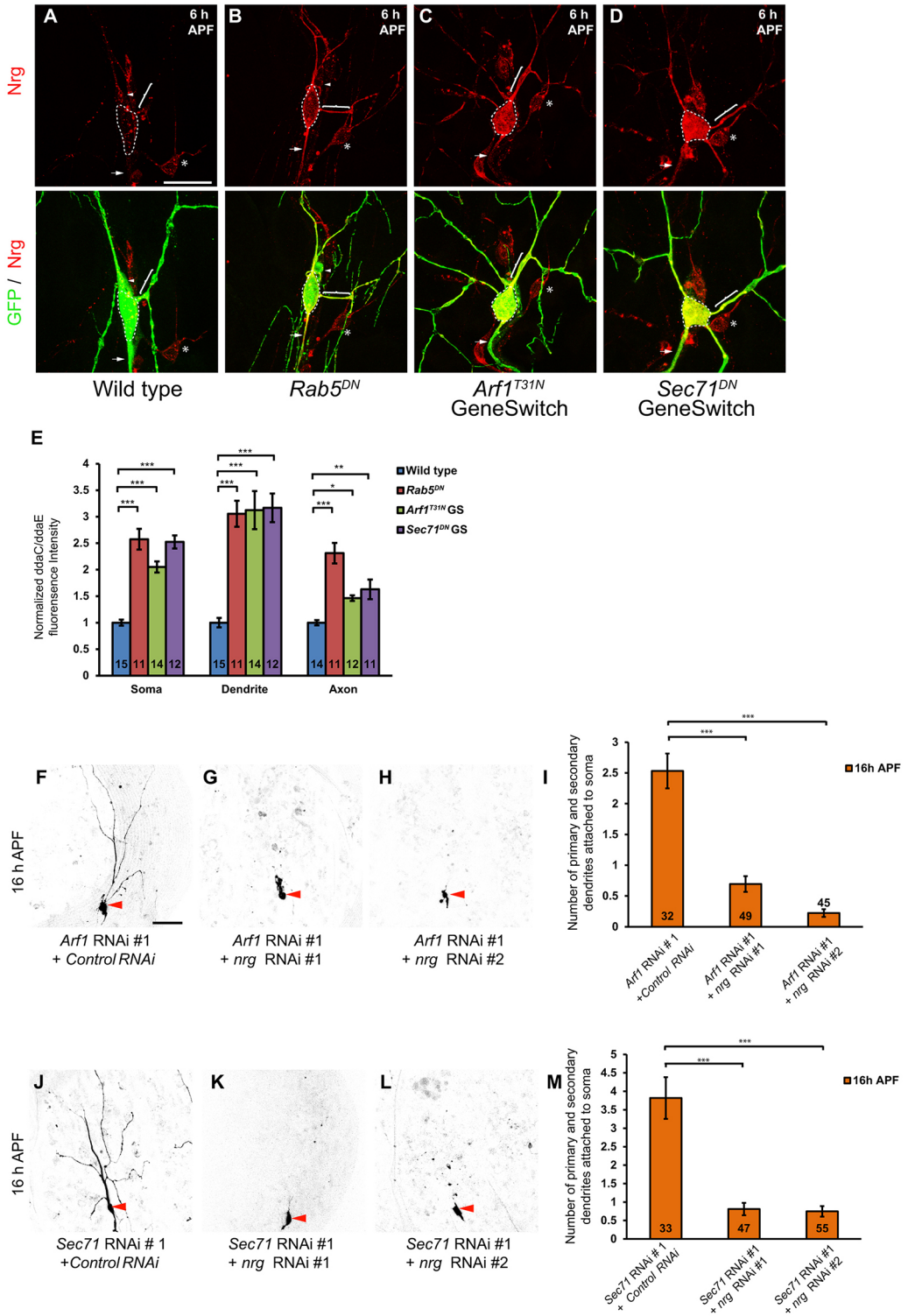

Fig. 7. The Arf1/Sec71-mediated secretory pathway is required for downregulation of the cell-adhesion molecule Nrg prior to dendrite pruning. (A-D) Distribution of Nrg in wild-type (A), *Rab5*^{DN} (B), *Arf1*^{T31N} (C) and *Sec71*^{DN} (D) ddaC neurons at 6 h APF. ddaC somas are marked by dashed lines, axons by arrows and proximal dendrites by curly brackets. ddaE somas are marked by asterisks. White arrowheads indicate apoptotic ddaF neurons. (E) Quantification of Nrg immunostaining intensity. (F-H) Dendrites of *Arf1* RNAi ddaC neurons co-expressing the control RNAi line (F), or *Nrg* RNAi #1 (G) or #2 (H) at 16 h APF. Red arrowheads indicate the ddaC somas. (I) Quantification of the average number of primary and secondary ddaC dendrites. (J-L) Dendrites of *Sec71* RNAi ddaC neurons co-expressing the control RNAi line (J), or *Nrg* RNAi #1 (K) or #2 (L) at 16 h APF. (M) Quantification of the average number of primary and secondary ddaC dendrites. Scale bars: 20 µm in A; 50 µm in F. Error bars represent s.e.m. N.S., not significant; **P*<0.05, ***P*<0.01, ****P*<0.001, as assessed by one-way ANOVA and Bonferroni test.

suppressed the dendrite severing defects in *Arf1* RNAi (Fig. 7G-I) or *Sec71* RNAi (Fig. 7K-M) ddaC neurons, further supporting the notion that, similar to Rab5, Arf1 and Sec71 facilitate Nrg endocytosis and degradation to promote dendrite pruning. There are at least two possibilities to explain how Arf1 and Sec71 regulate Nrg endocytosis: they act in a pathway that is either upstream of or

Development (2017) 144, 1851-1862 doi:10.1242/dev.146175

parallel to Rab5 to facilitate endocytosis. To distinguish these two possibilities, we created *Rab5* and *Arf1/Sec71* double mutants and examined their epistasis. Pulse expression of $Rab5^{DN}$ at the late larval stage via the gene-switch system led to pronounced accumulation of ubiquitylated protein deposits on two or three enlarged endosomes that were positively labelled with ubiquitin (Fig. S7B), the early endosomal marker Avl (Fig. S7C) and Nrg (Fig. S7C). These data suggest that Rab5 does not regulate the initial formation of early endosomes but is important for subsequent endosomal maturation as well as for Nrg downregulation (Zhang et al., 2014). By contrast, ubiquitin and Avl did not accumulate in $Arf1^{T31N}$ or $Sec71^{DN}$-expressing ddaC neurons (Fig. S7B,C). Importantly, $Arf1^{T31N}$ and $Rab5^{DN}$ double mutants did not exhibit any ubiquitylated aggregates (Fig. S7B) and Avl-positive enlarged endosomes (Fig. S7C) in ddaC neurons, resembling $Arf1^{T31N}$ single mutant neurons. Likewise, co-expression of $Sec71^{DN}$ and $Rab5^{DN}$ did not result in formation of ubiquitylated protein deposits (Fig. S7B) and Avl-positive endosomes (Fig. S7C), resembling $Sec71^{DN}$ mutant neurons. Thus, these epistatic data support the first possibility that Arf1 and Sec71 act upstream of Rab5 to facilitate initial formation of endosomes and robust endocytosis prior to dendrite pruning.

DISCUSSION

Sec71 is an important GEF for Arf1 in *Drosophila*

The small G protein Arf1 regulates vesicular trafficking in eukaryotes and is activated on *cis*-Golgi by the Gea1/GBF1 family of Arf1GEF or on *trans*-Golgi by the Sec7/BIG1 family (Cherfils, 2014). It has been reported that *Drosophila* Arf1 regulates hematopoietic niche maintenance, blood cell precursor differentiation *in vivo*, planar cell polarity and lamellipodium formation in S2 cells (Carvajal-Gonzalez et al., 2015; Humphreys et al., 2012; Khadilkar et al., 2014). Arf1 and other Golgi proteins were reported to exhibit upregulation of their transcripts in axon pruning of MB γ neurons during the larval-pupal transition (Hoopfer et al., 2008). In this study, we report an important role for Arf1 in regulating dendrite pruning of ddaC sensory neurons. We found that Arf1 puncta overlap with the *trans*-Golgi marker GalT and partially with the *cis*-Golgi marker GM130, suggesting that Arf1 is primarily localized on *trans*-Golgi in ddaC sensory neurons. A specific GEF for Arf1 has not been identified in *Drosophila*. Our *in vivo* and *in vitro* data provide compelling evidence that Sec71 is a GEF for Arf1 in *Drosophila*. First, Sec71 was colocalized with Arf1 on Golgi and their localizations were inter-dependent in ddaC neurons. Second, Sec71 preferentially bound to the GDP-bound form of Arf1 instead of GTP-bound form. Third, in the GEF assays Sec71 accelerated the release of GDP from Arf1. Fourth, both Arf1 and Sec71 are required for dendrite pruning, as loss of *Sec71* or *Arf1* led to comparable pruning defects in ddaC sensory neurons. Finally, the expression of Arf1 fully restored WP dendrite morphology and rescued the pruning defects in *Sec71* RNAi ddaC neurons. Thus, Sec71 is specifically required for the GDP-to-GTP exchange of Arf1.

Our structure-function analyses indicate that the DCB domain of Sec71 is important for its targeting on Golgi (Fig. S6). By contrast, another small GTPase, Arl1, was reported to bind to the N-terminal region of Sec71 (DCB and HUS1 domains) and to recruit Sec71 on *trans*-Golgi apparatus in *Drosophila* S2 cells; mammalian Arl1 is required for the recruitment of BIG1/2 (mammalian homologs of Sec71) on *trans*-Golgi (Christis and Munro, 2012). Unexpectedly, we found that mutant ddaC neurons derived from $arl1^{1}$, a null *arl1* mutant (Torres et al., 2014), did not exhibit delocalization of Sec71 or dendrite pruning defects in ddaC neurons (Fig. S1C), suggesting an Arl1-independent mechanism regulating Sec71 localization and function in ddaC sensory neurons.

The secretory pathway plays a novel and important role in governing neurite pruning

Extensive studies have attempted to understand roles of post-Golgi trafficking in outgrowth and elaboration of dendrites in growing neurons. Post-Golgi trafficking is polarized towards apical dendrites of rodent hippocampal neurons and selectively regulates the growth of dendrites (Horton and Ehlers, 2003; Horton et al., 2005). The dynamics of the Golgi outposts, mediated by the golgin Lava Lamp, dynein-dynactin complex and Leucine-rich repeat kinase (Lrrk), is important for dendrite growth in *Drosophila* class IV da neurons (Lin et al., 2015; Ye et al., 2007). Rab10, a small GTPase that mediates post-Golgi vesicle trafficking, regulates dendrite growth and branching of multi-dendritic sensory neurons in both *C. elegans* and *Drosophila* (Taylor et al., 2015; Zou et al., 2015).

In this study, we provide compelling evidence to demonstrate that post-Golgi trafficking plays a crucial role in proper dendrite pruning in sensory neurons. First, we identified that the key small GTPase Arf1, which is important for post-Golgi trafficking, regulates secretory vesicle biogenesis and dendrite pruning in sensory neurons during metamorphosis. Second, a Sec7-domain-containing protein Sec71 acts as a specific GEF for Arf1 and colocalizes with Arf1. Like Arf1, Sec71 is also an essential factor for regulating dendrite pruning. Third, given that both Arf1 and Sec71 also regulate dendrite growth and arborization in ddaC neurons, we further confirmed a crucial role for Arf1 and Sec71 in dendrite pruning using the gene-switch system. Pulse induction of $Arf1^{T31N}$ or $Sec71^{DN}$ at the middle third instar larval stage, when the complete larval dendrite arbors form in ddaC neurons, consistently caused much more severe dendrite pruning defects. These results highlight that the secretory pathway play separable roles in two distinct processes: dendrite growth and dendrite pruning. Arf1 was reported to regulate post-Golgi secretion by recruiting its downstream effectors, including the clathrin adaptors AP-1 and AP-3, and GGA (Cherfils, 2014). Post-Golgi trafficking pathways include the transport from Golgi to plasma membrane (exocyst complex mediated), from Golgi to early/sorting endosomes (AP-1 meditated), from Golgi to late endosomes (Golgi-localized gamma ear-containing Arf-binding protein or GGA mediated) as well as from Golgi to lysosomes (AP-3 mediated). It is conceivable that at least one of these post-Golgi trafficking routes is involved in dendrite pruning of sensory neurons.

Arf1/Sec71-dependent post-Golgi trafficking is a prerequisite for endocytosis and downregulation of Nrg prior to dendrite pruning

We have previously reported that Rab5/ESCRT-dependent endocytic pathways facilitate dendrite pruning by downregulating the L1-CAM Nrg in ddaC neurons during metamorphosis (Zhang et al., 2014). In MB γ neurons, the JNK pathway promotes axon pruning by downregulating another adhesion molecule: Fasciclin II (Bornstein et al., 2015). These studies suggest a general mechanism whereby cell-adhesion molecules are internalized and downregulated to destabilize dendrites and/or axons during neurite pruning. However, the mechanism that triggers Nrg endocytosis is poorly understood. In this study, we demonstrate that Arf1/Sec71-mediated secretory pathway promotes endocytosis and downregulates Nrg prior to dendrite pruning. First, although Nrg levels were strongly reduced prior to dendrite pruning, loss of

Development (2017) 144, 1851-1862 doi:10.1242/dev.146175

Arf1 or *Sec71* led to elevated levels of Nrg protein in dendrites, axons and soma, comparable with *Rab5* mutant neurons. Second, Nrg was no longer redistributed on FYVE-positive endosomes in *Arf1* or *Sec71* mutant ddaC neurons, suggesting a blockage of Nrg endocytosis. Third, whereas Rab5 mutant neurons exhibited robust ubiquitylated protein aggregates and enlarged endosomes, further removal of either Arf1 or Sec71 suppressed these *Rab5* mutant phenotypes, suggesting that the secretory pathway acts upstream of Rab5 to positively regulates endocytosis. Finally, knockdown of Nrg significantly suppressed the dendrite pruning defect in *Arf1* or *Sec71* mutant neurons, supporting the notion that the secretory pathway promotes Nrg endocytosis and downregulation. Thus, the secretory pathway not only secretes the cell-adhesion molecules to the dendrite surface and stabilize dendrites (Taylor et al., 2015; Zou et al., 2015), but also unexpectedly promotes the internalization and turnover of the adhesion molecules (this study). It is conceivable that, in response to an ecdysone pulse, the secretory pathway might be required to specifically secrete an as yet unidentified ligand to trigger robust endocytosis of the L1-CAM Nrg and thereby lead to degeneration of larval dendrites. Further studies may continue to elucidate what ligand or secreted protein promotes Nrg endocytosis.

MATERIALS AND METHODS

Fly strains

The fly stocks used in this study were maintained on standard food at 25°C. See supplementary Materials and Methods for further details of fly stocks used in this study.

MARCM analysis of ddaC neurons

We carried out MARCM clonal analysis, dendrite imaging and branch quantification as previously described (Kirilly et al., 2009). See supplementary Materials and Methods for further details.

RU486/mifepristone treatment for the gene-switch system

Wild-type and mutant embryos were collected at 3 h intervals and were reared on standard food to the middle 3rd instar larval stage before being transferred to the standard culture medium containing 240 µg/ml mifepristone (Sigma Aldrich, M8046).

Generation of *Sec71* mutants

We crossed $Sec71^{GS16990}$ flies with a fly strain carrying the $\Delta 2$–*3* transposase to induce imprecise excision as previously described (Kirilly et al., 2009). See supplementary Materials and Methods for further details.

Generation of *Arf1, Sec71* and other transgenes

The *Arf1* and *Sec71* full-length cDNA were PCR from EST LD24904 and LD29171 (DGRC) into Topo Entry and pDonor, respectively (Life Tech). The variants of *Sec71* and *Arf1* were generated by site mutagenesis (Agilent Tech). The cDNA fragment encoding the 1-100 amino acid region of rat ManII protein were used to generate ManII-Venus transgene (Bestgene). See supplementary Materials and Methods for further details.

Arf1 and Sec71 antibody production

The full-length Arf1 and the 60-345 amino acid fragment of Sec71 were used for their respective antibody generation. See supplementary Materials and Methods for further details.

Immunohistochemistry and antibodies

Pupae or larvae were dissected in PBS and fixed with 4% formaldehyde for 20 min. The primary antibodies and Cy3-, Cy5- or fluorescein isothiocyanate (FITC)-conjugated secondary antibodies were used for immunohistochemistry. Mounting was performed in VectaShield mounting medium, and the samples were directly visualized by confocal microscopy. See supplementary Materials and Methods for further details.

Co-immunoprecipitation and GST pull-down assay

Transfected S2 cells were homogenized with the lysis buffer. The supernatants were used for immunoprecipitation, followed by incubation with protein A/G beads (Pierce Chemical). Protein A/G beads were washed four times. Bound proteins were separated by SDS-PAGE and analyzed by western blotting with anti-Myc, anti-Flag HRP-conjugated antibody. See supplementary Materials and Methods for further details.

Trafficking assay

The fillets were incubated with rat monoclonal anti-CD8α (1:100, CALTAG Laboratories) in PBS and washed three times with PBS in the detergent-free condition. See supplementary Materials and Methods for further details.

In vitro guanine nucleotide exchange assay

We carried out the *in vitro* guanine nucleotide exchange assays as previously described (Mahajan et al., 2013). GST fusion proteins for the Sec7 domain of Sec71 (amino acids 554-790), its dominant negative form (E-K) and Sec7 domain of human BIG1 were expressed using the GST expression vector pGEB. 6×His-tagged $Arf1^{WT}$ and 6×His-tagged $Arl1^{WT}$ were expressed via the vector pET37b. See supplementary Materials and Methods for further details.

Quantification of immunolabeling

We quantified the immunolabelling intensities of Nrg at 6 h APF, as described previously (Zhang et al., 2014). One-way ANOVA and Bonferroni tests were used for comparisons between different conditions (*P<0.05, **P<0.01, ***P<0.001; n.s., not significant). See supplementary Materials and Methods for further details.

Quantification of ddaC dendrites

Live confocal images of ddaC neurons were shown at the WP stage and 16 h APF. Statistical significance was determined using either two-tailed Student's *t*-test (two samples) or one-way ANOVA and Bonferroni test (multiple samples) (*P<0.05, **P<0.01, ***P<0.001; n.s., not significant). See supplementary Materials and Methods for further details.

Acknowledgements

We thank H. Bellen, R. L. Borgne, E. Chen, J. Eissenberg, M. Gonzalez-Gaitan, T. Harris, S. Hayashi, Y. Jan, J. Kennison, A. Kolodkin, S. Luschnig, M. Metzstein, E. Olson, T. Schwarz, T. Uemura, the Bloomington Stock Center (BSC), DSHB (University of Iowa), the Kyoto Stock Center (Japan) and the VDRC (Austria) for generously providing antibodies and fly stocks. We thank members of the Yu laboratory for helpful assistance and discussion.

Competing interests

The authors declare no competing or financial interests.

Author contributions

Conceptualization: Y.W., F.Y.; Methodology: Y.W., H.Z., M.S., Y.-C.L., L.L., F.Y.; Software: Y.W., F.Y.; Validation: Y.W., H.Z., M.S., L.L., F.Y.; Formal analysis: Y.W., M.S., Y.L., L.L., F.Y.; Investigation: Y.W., H.Z., M.S., L.L., F.Y.; Resources: Y.W., L.L., F.Y.; Data curation: Y.W., H.Z., M.S., F.Y.; Writing - original draft: Y.W., F.Y.; Writing - review & editing: F.Y.; Visualization: Y.W., H.Z., L.L., F.Y.; Supervision: Y.-C.L., L.L., F.Y.; Project administration: F.Y.; Funding acquisition: F.Y.

Funding

This work was funded by an National University of Singapore Graduate School for Integrative Sciences and Engineering postgraduate scholarship (NGS-A0113474L to Y.W.); by Ministry of Education – Singapore grants (AcRF Tier2 MOE-T2-1-153 R-154-000-598-112 to Y.-C.L.; and AcRF Tier2 MOE2015-T2-2-073, AcRF Tier1 RG132/15 and AcRF Tier1 RG48/13 to L.L.); and by a Temasek Life Sciences Laboratory internal grant (TLL-2040 to F.Y.).

Supplementary information

Supplementary information available online at
http://dev.biologists.org/lookup/doi/10.1242/dev.146175.supplemental

References

Aridor, M. and Fish, K. N. (2009). Selective targeting of ER exit sites supports axon development. *Traffic* **10**, 1669-1684.

Development (2017) 144, 1851-1862 doi:10.1242/dev.146175

Bagri, A., Cheng, H.-J., Yaron, A., Pleasure, S. J. and Tessier-Lavigne, M. (2003). Stereotyped pruning of long hippocampal axon branches triggered by retraction inducers of the semaphorin family. *Cell* **113**, 285-299.

Bornstein, B., Zahavi, E. E., Gelley, S., Zoosman, M., Yaniv, S. P., Fuchs, O., Porat, Z., Perlson, E. and Schuldiner, O. (2015). Developmental axon pruning requires destabilization of cell adhesion by JNK signaling. *Neuron* **88**, 926-940.

Carvajal-Gonzalez, J. M., Balmer, S., Mendoza, M., Dussert, A., Collu, G., Roman, A.-C., Weber, U., Ciruna, B. and Mlodzik, M. (2015). The clathrin adaptor AP-1 complex and Arf1 regulate planar cell polarity in vivo. *Nat. Commun.* **6**, 6751.

Cherfils, J. (2014). Arf GTPases and their effectors: assembling multivalent membrane-binding platforms. *Curr. Opin. Struct. Biol.* **29**, 67-76.

Christis, C. and Munro, S. (2012). The small G protein Arl1 directs the trans-Golgi-specific targeting of the Arf1 exchange factors BIG1 and BIG2. *J. Cell Biol.* **196**, 327-335.

Dascher, C. and Balch, W. E. (1994). Dominant inhibitory mutants of ARF1 block endoplasmic reticulum to Golgi transport and trigger disassembly of the Golgi apparatus. *J. Biol. Chem.* **269**, 1437-1448.

D'Souza-Schorey, C. and Chavrier, P. (2006). ARF proteins: roles in membrane traffic and beyond. *Nat. Rev. Mol. Cell Biol.* **7**, 347-358.

Ferland, R. J., Batiz, L. F., Neal, J., Lian, G., Bundock, E., Lu, J., Hsiao, Y.-C., Diamond, R., Mei, D., Banham, A. H. et al. (2009). Disruption of neural progenitors along the ventricular and subventricular zones in periventricular heterotopia. *Hum. Mol. Genet.* **18**, 497-516.

Garcia-Mata, R., Szul, T., Alvarez, C. and Sztul, E. (2003). ADP-ribosylation factor/COPI-dependent events at the endoplasmic reticulum-Golgi interface are regulated by the guanine nucleotide exchange factor GBF1. *Mol. Biol. Cell* **14**, 2250-2261.

Gillingham, A. K. and Munro, S. (2007). The small G proteins of the Arf family and their regulators. *Annu. Rev. Cell Dev. Biol.* **23**, 579-611.

Grueber, W. B., Ye, B., Moore, A. W., Jan, L. Y. and Jan, Y. N. (2003). Dendrites of distinct classes of Drosophila sensory neurons show different capacities for homotypic repulsion. *Curr. Biol.* **13**, 618-626.

Hoopfer, E. D., Penton, A., Watts, R. J. and Luo, L. (2008). Genomic analysis of Drosophila neuronal remodeling: a role for the RNA-binding protein Boule as a negative regulator of axon pruning. *J. Neurosci.* **28**, 6092-6103.

Horton, A. C. and Ehlers, M. D. (2003). Neuronal polarity and trafficking. *Neuron* **40**, 277-295.

Horton, A. C. and Ehlers, M. D. (2004). Secretory trafficking in neuronal dendrites. *Nat. Cell Biol.* **6**, 585-591.

Horton, A. C., Rácz, B., Monson, E. E., Lin, A. L., Weinberg, R. J. and Ehlers, M. D. (2005). Polarized secretory trafficking directs cargo for asymmetric dendrite growth and morphogenesis. *Neuron* **48**, 757-771.

Humphreys, D., Liu, T., Davidson, A. C., Hume, P. J. and Koronakis, V. (2012). The Drosophila Arf1 homologue Arf79F is essential for lamellipodium formation. *J. Cell Sci.* **125**, 5630-5635.

Jafar-Nejad, H., Andrews, H. K., Acar, M., Bayat, V., Wirtz-Peitz, F., Mehta, S. Q., Knoblich, J. A. and Bellen, H. J. (2005). Sec15, a component of the exocyst, promotes notch signaling during the asymmetric division of Drosophila sensory organ precursors. *Dev. Cell* **9**, 351-363.

Kanamori, T., Togashi, K., Koizumi, H. and Emoto, K. (2015a). Dendritic remodeling: lessons from invertebrate model systems. *Int. Rev. Cell Mol. Biol.* **318**, 1-25.

Kanamori, T., Yoshino, J., Yasunaga, K., Dairyo, Y. and Emoto, K. (2015b). Local endocytosis triggers dendritic thinning and pruning in Drosophila sensory neurons. *Nat. Commun.* **6**, 6515.

Khadilkar, R. J., Rodrigues, D., Mote, R. D., Sinha, A. R., Kulkarni, V., Magadi, S. S. and Inamdar, M. S. (2014). ARF1-GTP regulates Asrij to provide endocytic control of Drosophila blood cell homeostasis. *Proc. Natl. Acad. Sci. USA* **111**, 4898-4903.

Kirilly, D., Gu, Y., Huang, Y., Wu, Z., Bashirullah, A., Low, B. C., Kolodkin, A. L., Wang, H. and Yu, F. (2009). A genetic pathway composed of Sox14 and Mical governs severing of dendrites during pruning. *Nat. Neurosci.* **12**, 1497-1505.

Kuo, C. T., Jan, L. Y. and Jan, Y. N. (2005). Dendrite-specific remodeling of Drosophila sensory neurons requires matrix metalloproteases, ubiquitin-proteasome, and ecdysone signaling. *Proc. Natl. Acad. Sci. USA* **102**, 15230-15235.

Lee, T., Lee, A. and Luo, L. (1999). Development of the Drosophila mushroom bodies: sequential generation of three distinct types of neurons from a neuroblast. *Development* **126**, 4065-4076.

Lin, C.-H., Li, H., Lee, Y.-N., Cheng, Y.-J., Wu, R.-M. and Chien, C.-T. (2015). Lrrk regulates the dynamic profile of dendritic Golgi outposts through the golgin Lava lamp. *J. Cell Biol.* **210**, 471-483.

Lippincott-Schwartz, J., Roberts, T. H. and Hirschberg, K. (2000). Secretory protein trafficking and organelle dynamics in living cells. *Annu. Rev. Cell Dev. Biol.* **16**, 557-589.

Luo, L. and O'Leary, D. D. M. (2005). Axon retraction and degeneration in development and disease. *Annu. Rev. Neurosci.* **28**, 127-156.

Mahajan, D., Boh, B. K., Zhou, Y., Chen, L., Cornvik, T. C., Hong, W. and Lu, L. (2013). Mammalian Mon2/Ysl2 regulates endosome-to-Golgi trafficking but possesses no guanine nucleotide exchange activity toward Arl1 GTPase. *Sci. Rep.* **3**, 3362.

O'Leary, D. D. M. and Koester, S. E. (1993). Development of projection neuron types, axon pathways, and patterned connections of the mammalian cortex. *Neuron* **10**, 991-1006.

Peng, Y., Lee, J., Rowland, K., Wen, Y., Hua, H., Carlson, N., Lavania, S., Parrish, J. Z. and Kim, M. D. (2015). Regulation of dendrite growth and maintenance by exocytosis. *J. Cell Sci.* **128**, 4279-4292.

Pfenninger, K. H. (2009). Plasma membrane expansion: a neuron's Herculean task. *Nat. Rev. Neurosci.* **10**, 251-261.

Riccomagno, M. M. and Kolodkin, A. L. (2015). Sculpting neural circuits by axon and dendrite pruning. *Annu. Rev. Cell Dev. Biol.* **31**, 779-805.

Schuldiner, O. and Yaron, A. (2015). Mechanisms of developmental neurite pruning. *Cell. Mol. Life Sci.* **72**, 101-119.

Sheen, V. L., Ganesh, V. S., Topcu, M., Sebire, G., Bodell, A., Hill, R. S., Grant, P. E., Shugart, Y. Y., Imitola, J., Khoury, S. J. et al. (2004). Mutations in ARFGEF2 implicate vesicle trafficking in neural progenitor proliferation and migration in the human cerebral cortex. *Nat. Genet.* **36**, 69-76.

Tapia, J. C., Wylie, J. D., Kasthuri, N., Hayworth, K. J., Schalek, R., Berger, D. R., Guatimosim, C., Seung, H. S. and Lichtman, J. W. (2012). Pervasive synaptic branch removal in the mammalian neuromuscular system at birth. *Neuron* **74**, 816-829.

Taylor, C. A., Yan, J., Howell, A. S., Dong, X. and Shen, K. (2015). RAB-10 regulates dendritic branching by balancing dendritic transport. *PLoS Genet.* **11**, e1005695.

Torres, I. L., Rosa-Ferreira, C. and Munro, S. (2014). The Arf family G protein Arl1 is required for secretory granule biogenesis in Drosophila. *J. Cell Sci.* **127**, 2151-2160.

Truman, J. W. (1990). Metamorphosis of the central nervous system of Drosophila. *J. Neurobiol.* **21**, 1072-1084.

Williams, D. W. and Truman, J. W. (2005). Cellular mechanisms of dendrite pruning in Drosophila: insights from in vivo time-lapse of remodeling dendritic arborizing sensory neurons. *Development* **132**, 3631-3642.

Ye, B., Zhang, Y., Song, W., Younger, S. H., Jan, L. Y. and Jan, Y. N. (2007). Growing dendrites and axons differ in their reliance on the secretory pathway. *Cell* **130**, 717-729.

Yu, F. and Schuldiner, O. (2014). Axon and dendrite pruning in Drosophila. *Curr. Opin. Neurobiol.* **27**, 192-198.

Zhang, H., Wang, Y., Wong, J. J. L., Lim, K.-L., Liou, Y.-C., Wang, H. and Yu, F. (2014). Endocytic pathways downregulate the L1-type cell adhesion molecule neuroglian to promote dendrite pruning in Drosophila. *Dev. Cell* **30**, 463-478.

Zou, W., Yadav, S., DeVault, L., Jan, Y. N. and Sherwood, D. R. (2015). RAB-10-dependent membrane transport is required for dendrite arborization. *PLoS Genet.* **11**, e1005484.

Supplemental Information

Sec71 functions as a GEF for the small GTPase Arf1 to govern dendrite pruning of *Drosophila* sensory neurons

Yan Wang[1,2], Heng Zhang[1], Meng Shi[3], Yih-Cherng Liou[1,2], Lei Lu[3], Fengwei Yu[1,2,4,*]

Development • Supplementary information

Figure S1

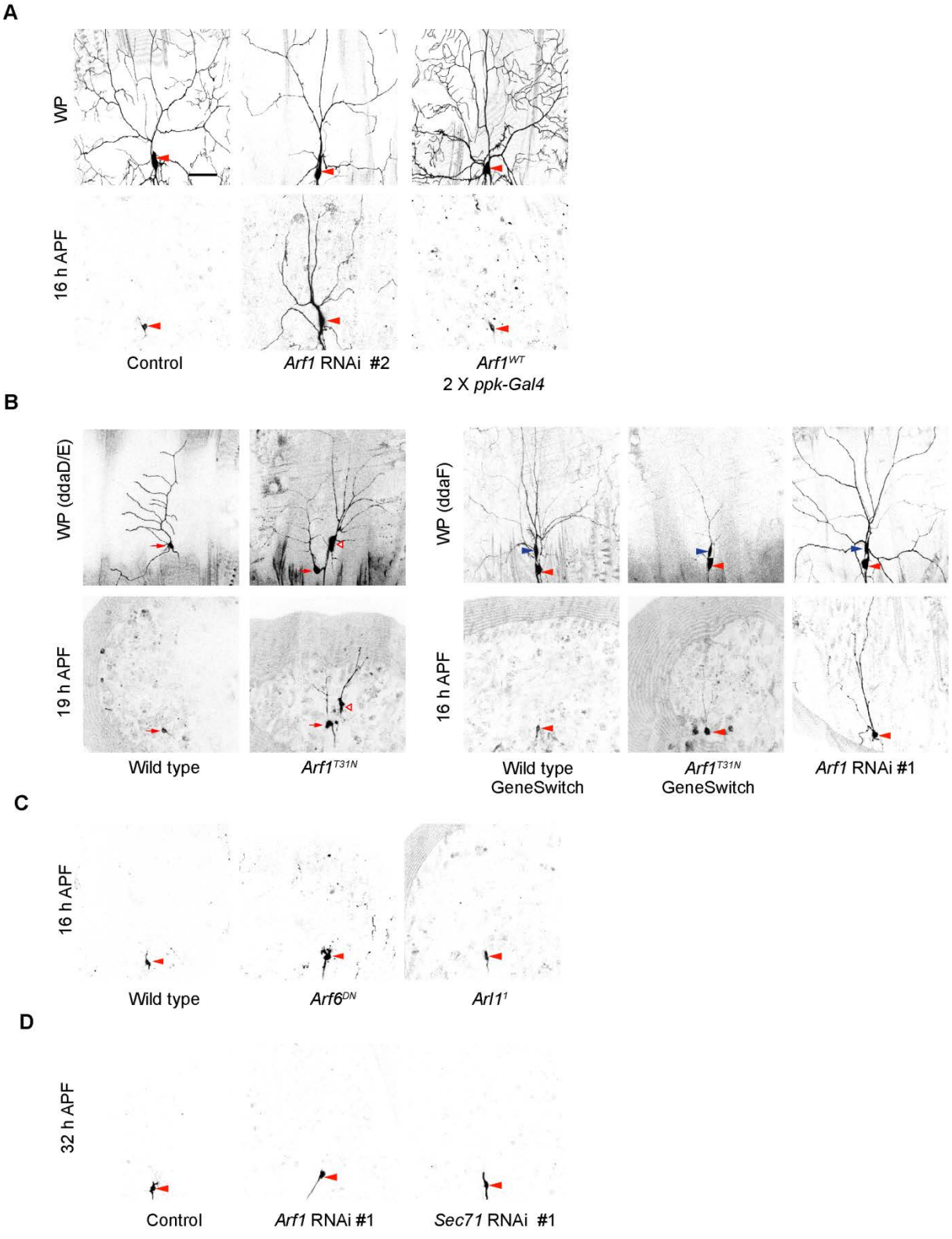

Development • Supplementary information

Figure S1. Arf1 is required for dendrite pruning in da sensory neurons.

(A-D) Live confocal images of ddaC or ddaD/E neurons expressing mCD8-GFP at WP stage, 16 h or 19 h APF. (A) While the control neurons that expressed an irrelevant RNAi line pruned all the dendrites, ddaC neurons overexpressing *Arf1* RNAi #2 by *ppk-Gal4* exhibited simple dendrite arbors at WP stage and dendrite pruning defects at 16 h APF. $Arf1^{WT}$-expressing ddaC neurons by two copies of *ppk-Gal4* driver at WP stage exhibited normal dendrite morphology and pruned their larval dendrites at 16 h APF. Red arrowheads point to the ddaC somas. (B) While wild-type class I ddaD/ddaE neurons pruned their larval dendrites at 19 h APF, $Arf1^{T31N}$ mutant ddaD and ddaE clones retained some of their larval dendrites at the same time point. Red arrows point to the ddaD somas and open arrowheads to the ddaE somas. Wild-type ddaF underwent apoptosis and disappeared at 16 h APF. Similarly, $Arf1^{T31N}$ ddaF labelled by GSG2295-driven mCD8-GFP and *Arf1* RNAi #1 mutant ddaF neurons were also removed at 16 h APF. Red arrowheads point to the ddaC somas, and blue arrowheads point to the ddaF somas. (C) Dendrites of $Arf6^{DN}$-expressing ddaC neurons and $Arl1^{1}$ MARCM ddaC clones (n=5) were pruned at 16 h APF, similar to the wild-type controls. (D) Similar to the control RNAi-expressing ddaC neurons, ddaC neurons overexpressing *Arf1* RNAi #1 (n=14) and *Sec71* RNAi #1 (n=12) by *ppk-Gal4* pruned all the dendrites at 32 h APF. Red arrowheads point to the ddaC somas. Scale bar in (A) represents 50 μm. See genotypes in Supplemental list of fly strains.

Development • Supplementary information

Figure S2

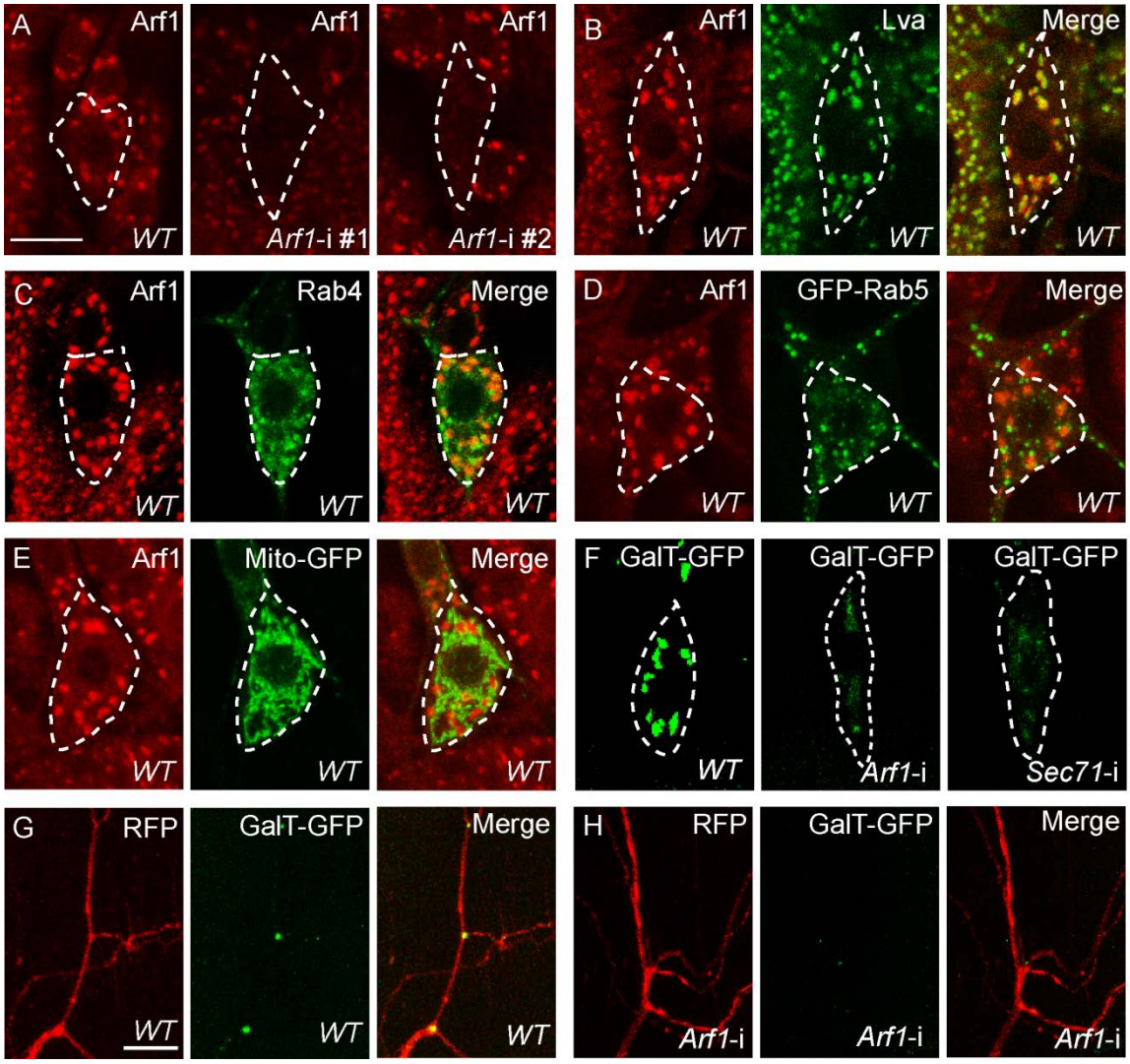

Development • Supplementary information

Figure S2. Arf1 does not localize on endosomes and mitochondria in ddaC sensory neurons.

(A-E) Confocal images of wild-type and mutant ddaC neurons at the late wL3 stage immunostained with anti-Arf1 or anti-Lva. ddaC somas are marked by dashed lines. (A) While Arf1 exhibited punctate structures in wild-type ddaCs, Arf1 staining in *Arf1* #1 RNAi or *Arf1* #2 RNAi ddaC neurons was abolished, verifying the specificity of the anti-Arf1 antibody. (B) Arf1-positive puncta (in red) largely co-localized with the Golgi marker Lva (in green) in wild-type ddaC somas. (C) Arf1-positive puncta (in red) did not overlap with the recycling endosomal marker Rab4-mRFP (in green) in wild-type ddaC neurons. (D) Arf1-positive puncta (in red) did not overlap with the early endosomal marker GFP-Rab5 (in green) in wild-type ddaC neurons. (E) Arf1-positive puncta (in red) did not overlap with the mitochondrial marker Mito-GFP (in green) in wild-type ddaC neurons. (F-H) Live confocal images of ddaC neurons expressing GalT-GFP and mCD8-RFP at WP stage. (F) GalT-GFP signals in soma were largely disrupted in *Arf1* RNAi and *Sec71* RNAi-expressing ddaC neurons. (G-H) GalT-GFP-positive dendritic Golgi outposts were disrupted in *Arf1* RNAi ddaC neurons (H), compared to those in wild-type ddaC neurons (G). Scale bars in (A) and (G) represent 10 μm. See genotypes in Supplemental list of fly strains.

Development • Supplementary information

Figure S3

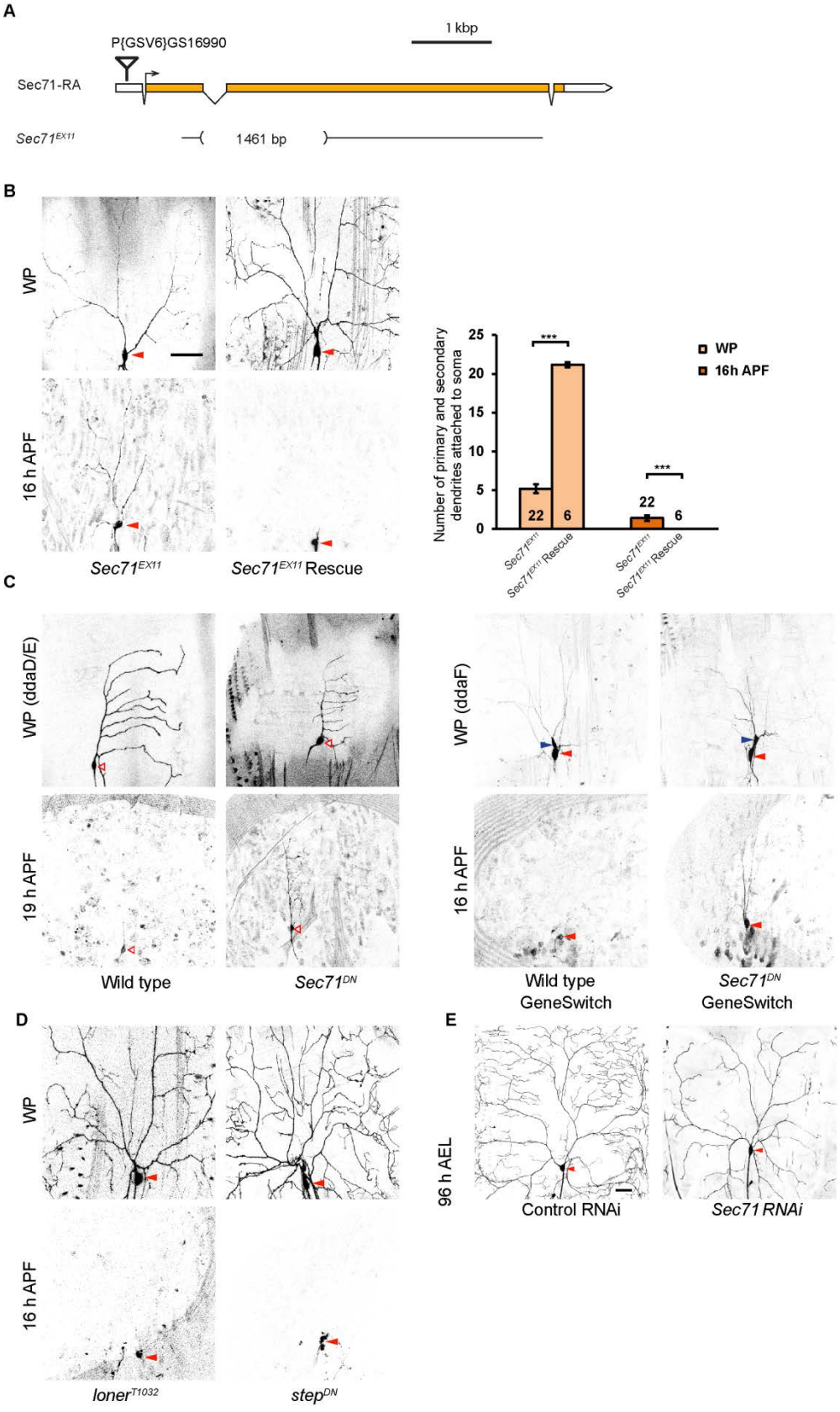

Development • Supplementary information

Figure S3. Sec71 is crucial for the regulation of dendrite pruning in sensory neurons.

(A) A schematic diagram of the *Sec71* gene and the deleted region of the $Sec71^{Ex11}$ mutant. The P-element insertion P{GSV6}GS16990, which is inserted in the first exon of the gene, was used to generate imprecise excision mutants. The start site of the *Sec71* open reading frame is shown in an arrow. (B-E) Live confocal images of ddaC or ddaD/E neurons expressing mCD8-GFP at wL3, WP, 16 h or 19 h APF stages. (B) $Sec71^{Ex11}$ MARCM ddaC clones exhibited simple arbors at WP stage and pruning defects at 16 h APF. Both dendrite morphological defects and pruning defects could be rescued by expressing full-length Sec71 protein in $Sec71^{Ex11}$ MARCM ddaC neurons. Red arrowheads point to the ddaC somas. Quantification of the average number of primary and secondary ddaC dendrites. Error bars represent S.E.M.. ***$p < 0.001$ as assessed by two-tailed Student's T test. (C) While wild-type class I ddaD/ddaE neurons pruned their larval dendrites at 19 h APF, $Sec71^{DN}$ ddaD or ddaE MARCM mutant clones failed to prune their larval dendrites at 19 h APF. Open arrowheads point to the ddaE somas. Wild-type ddaFs underwent apoptosis and were gone by 16 h APF. Similarly, $Sec71^{DN}$ ddaFs labelled by GSG2295-driven mCD8-GFP also underwent apoptosis by 16 h APF. Red arrowheads point to the ddaC somas, and blue arrowheads point to the ddaF somas. (D) Dendrites of $loner^{T1032}$ MARCM and $Step^{DN}$-expressing ddaC neurons were removed by 16 h APF. (E) While control RNAi-expressing ddaC neurons exhibited complex arbors at 96 h AEL, *Sec71* RNAi-expressing ddaC neurons exhibited simplified arbors. Red arrowheads point to the ddaC somas. Scale bar in (B) and (E) represents 50 μm. See genotypes in Supplemental list of fly strains.

Development • Supplementary information

Figure S4

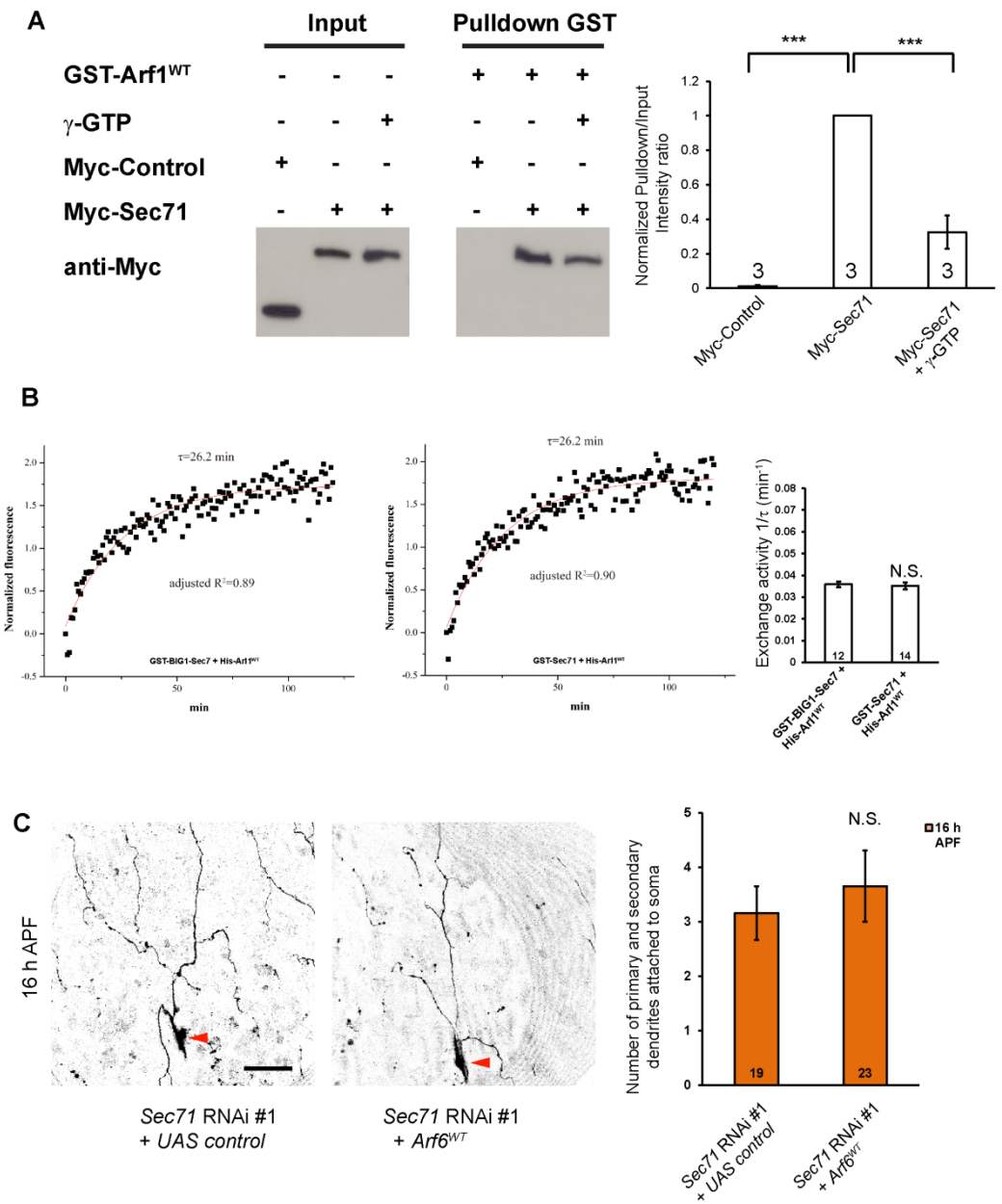

Development • Supplementary information

Figure S4. Sec71 is an Arf1GEF that preferentially interacts with GDP-bound Arf1.

(A) GST-Arf1^{WT} was associated with Myc-Sec71 but not with the Myc-tagged control protein, and this association was reduced in the presence of γ-GTP (n=3). Myc-tagged Sec71 and control protein were transfected and expressed in S2 cells. Error bars represent S.E.M.. ***p < 0.001 as assessed by one-way ANOVA and Bonferroni test. (B) Kinetics of fluorescence increases of GTP analog. Incubation of GST-tagged Sec7 domain of Sec71 (Sec71) led to slow kinetics towards Arl1, similar to the control GST-tagged Sec7 domain of hBIG1. Quantification of the exchange activity reflected by inverse of time constant, 1/τ value. N.S. not significant, as assessed by a Student's T-test. (C) The expression of Arf6^{WT} was unable to suppress the pruning defects in *Sec71* RNAi ddaC neurons at 16 h APF. Red arrowheads point to the ddaC somas. Quantification of the average number of primary and secondary ddaC dendrites. Scale bar in (C) represents 50 μm. Error bars represent S.E.M.. N.S. not significant, as assessed by two-tailed Student's T test. See genotypes in Supplemental list of fly strains.

Development • Supplementary information

Figure S5

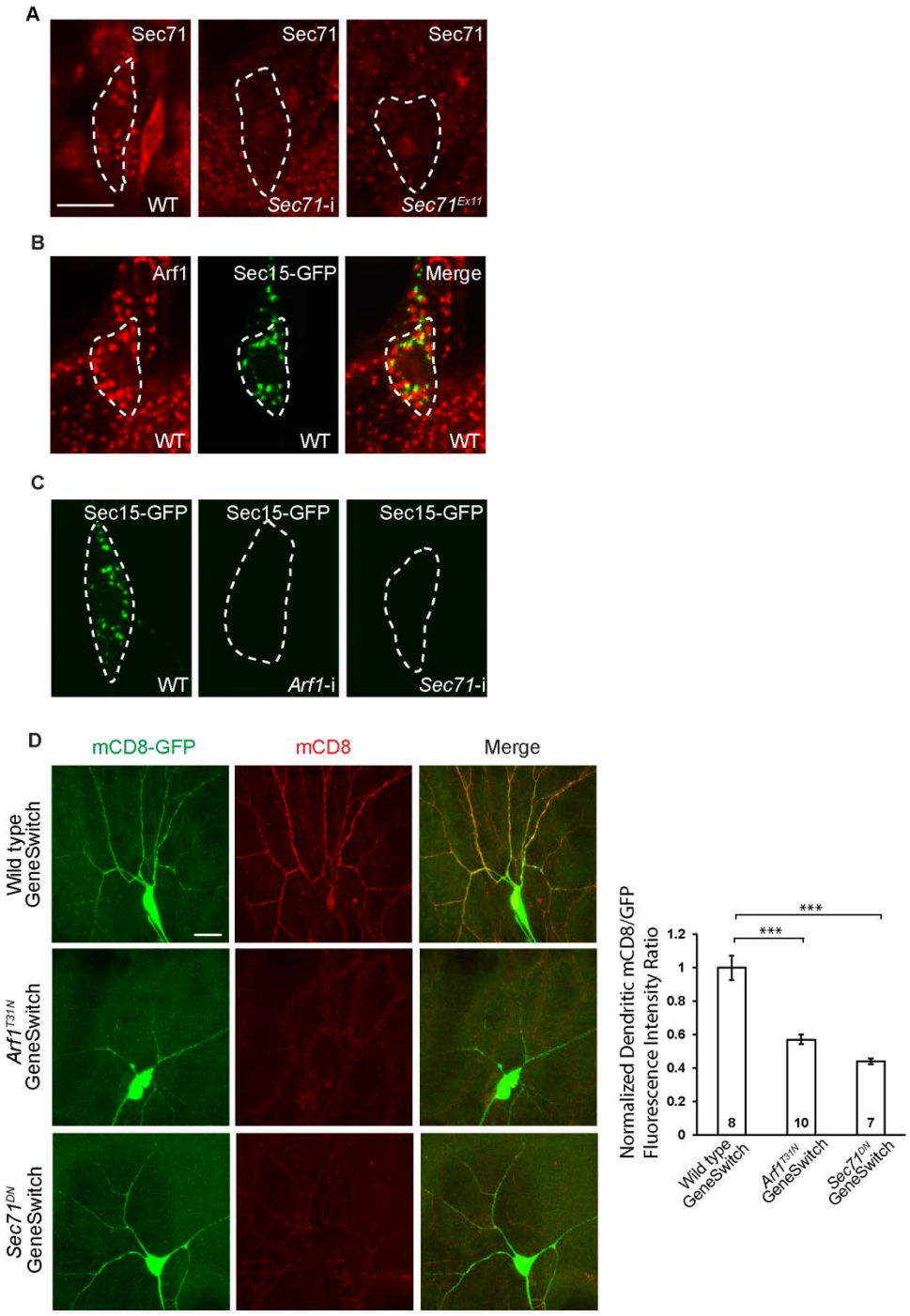

Development • Supplementary information

Figure S5. Arf1 and Sec71 regulate protein transport to the dendrite surface.

(A) Confocal images of wild-type and mutant ddaC neurons at the late wL3 stage immunostained with anti-Sec71. ddaC somas are marked by dashed lines. While Sec71 was distributed as punctate structures in wild-type ddaCs, Sec71 signals were completely abolished in *Sec71* RNAi #1 ddaC neurons and $Sec71^{Ex11}$ MARCM clones, verifying the specificity of the Sec71 antibody. (B) Sec15-positive puncta were localized adjacent to or partially colocalized with the Arf1-positive Golgi apparatus in wild-type ddaC neurons. (C) Sec15-GFP puncta were disrupted in *Arf1* RNAi and *Sec71* RNAi knockdown ddaC neurons, compared to the wild type. ddaC somas are marked by dashed lines. (D) mCD8 signals on the surface of the dendrites in wild-type ddaC neurons were detected by the antibody against its extracellular epitope in the detergent-free condition. However, the mCD8 signals were greatly reduced in $Sec71^{DN}$, and $Arf1^{T31N}$ expressing ddaC neurons. The graph represents quantification of normalized dendritic mCD8/GFP intensity. The scale bars represent 10 μm in (A) and 20 μm in (D). Error bars represent S.E.M.. ***$p < 0.001$ as assessed by one-way ANOVA and Bonferroni test. See genotypes in Supplemental list of fly strains.

Development • Supplementary information

Figure S6

A

Sec71 antigen		Dendrite Morpology	Dendrite Pruning Defect	TGN localization
DCB HUS Sec7 HDS1 HDS2 HDS3 HDS4	Sec71	Fully restored	Fully rescued	Yes
HUS Sec7 HDS1 HDS2 HDS3 HDS4	ΔDCB	Partially restored	Not rescued	No
DCB Sec7 HDS1 HDS2 HDS3 HDS4	ΔHUS	Further reduced	N.A.	Yes
DCB HUS Sec7 HDS2 HDS3 HDS4	ΔHDS1	Further reduced	N.A.	Yes
DCB HUS Sec7 HDS1	ΔHDS2-4	Fully restored	Fully rescued	Yes
DCB HUS Sec7 HDS1 HDS2	ΔHDS3-4	Fully restored	Fully rescued	Yes
DCB HUS Sec7 HDS1 HDS2 HDS3	ΔHDS4	Fully restored	Fully rescued	Yes

B

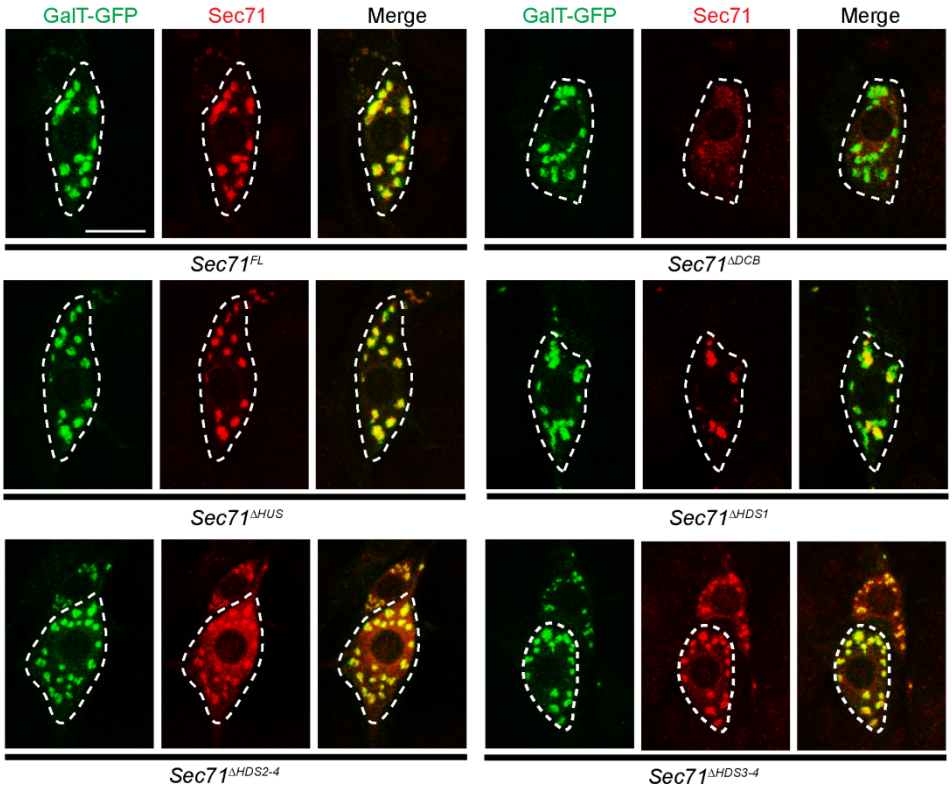

Development • Supplementary information

Figure S6. Structure-function analysis of the Sec71 protein.

(A) A summary of structure-function analysis of Sec71. Sec71 contains multiple domains: Dimerization/Cyclophilin Binding domain (DCB), Homology Upstream of Sec7 domain (HUS), Sec7 domain and Homology Downstream of Sec7 domain (HDS). (B) Confocal images of ddaC neurons at the late wL3 stage immunostained with anti-Sec71. Similar to full-length RNAi-resistant Sec71, Sec71$^{\Delta HUS}$, Sec71$^{\Delta HDS1}$, Sec71$^{\Delta HDS2\text{-}4}$ and Sec71$^{\Delta HDS3\text{-}4}$, but not Sec71$^{\Delta DCB}$, were localized on Golgi compartments labelled by GalT-GFP in ddaC neurons. Scale bar in (B) represents 10 μm. See genotypes in Supplemental list of fly strains.

Development • Supplementary information

Figure S7

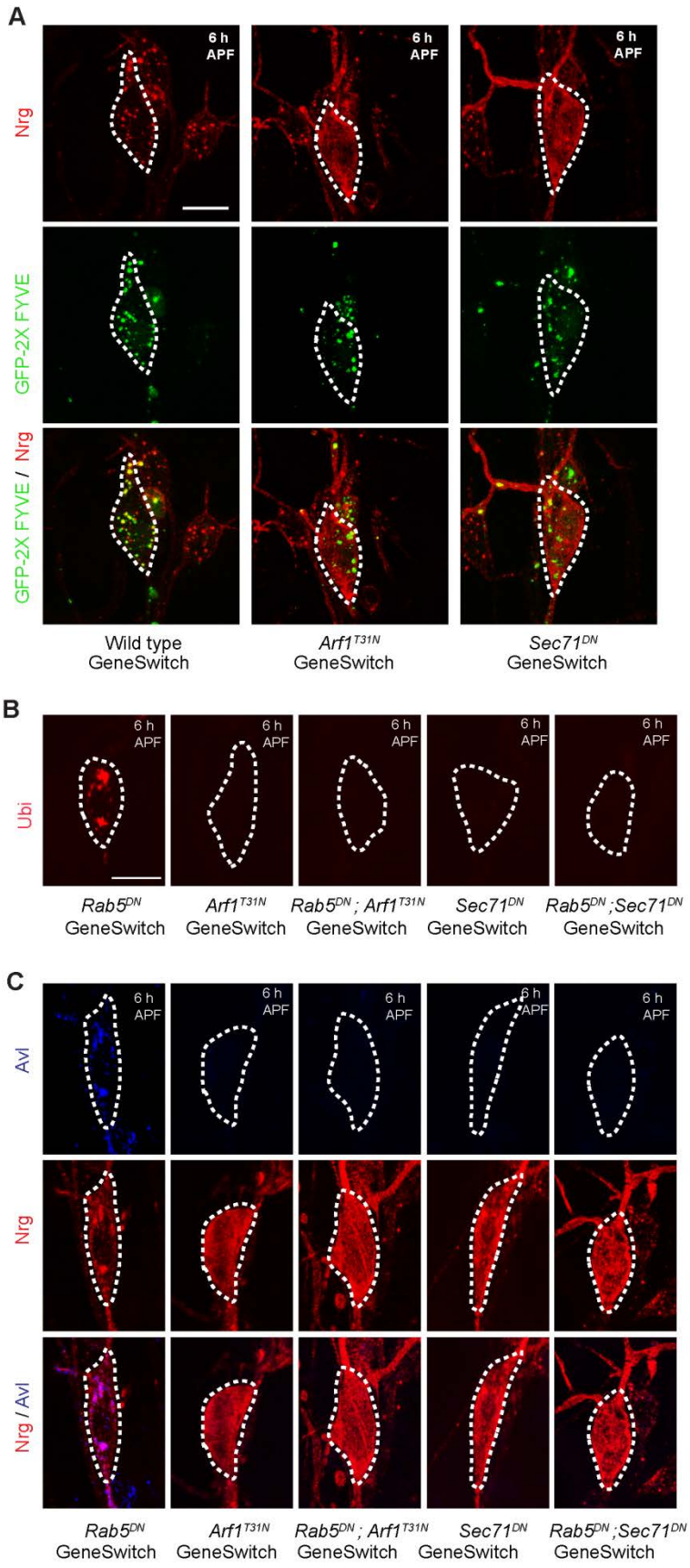

Development • Supplementary information

Figure S7. Arf1/Sec71-mediated secretory pathway is required for downregulation of the cell adhesion molecule Nrg prior to dendrite pruning

(A-C) Confocal images of ddaC neurons at 6 h APF stage immunostained for anti-Nrg (in red), anti-Ubiquitin (in red) or anti-Avl (in blue). (A) While Nrg proteins in wild-type ddaC neurons were redistributed to the early endosome labelled by GFP-2xFYVE at 6 h APF, Nrg in $Arf1^{T31N}$ or $Sec71^{DN}$-expressing ddaC neurons did not co-localize with those GFP-2xFYVE puncta and remained on the plasma membrane. (B) 2-3 ubiquitinated protein deposits were accumulated in $Rab5^{DN}$ expressing ddaC neurons but not in $Arf1^{T31N}$, $Rab5^{DN}$ and $Arf1^{T31N}$ co-expressing, $Sec71^{DN}$, or $Rab5^{DN}$ and $Sec71^{DN}$ co-expressing ddaC neurons at 6 h APF. (C) Avl/Nrg-positive aberrant endosomes were present in $Rab5^{DN}$ expressing ddaC neurons but absent in $Arf1^{T31N}$-expressing, $Rab5^{DN}$ and $Arf1^{T31N}$-co-expressing, $Sec71^{DN}$-expressing, or $Rab5^{DN}$ and $Sec71^{DN}$-co-expressing ddaC neurons at 6 h APF. ddaC somas are marked by dashed lines. The scale bars in (A) and (B) represent 10 μm. See genotypes in Supplemental list of fly strains.

Development • Supplementary information

Supplemental Material and Methods

Fly Strains

The following fly stocks were used in this study: *UAS-Rab5*^{DN} (M. Gonzalez-Gaitan)(Wucherpfennig et al., 2003), *UAS-GFP-Rab5* (M. Gonzalez-Gaitan)(Wucherpfennig et al., 2003), *UAS-Mical*$^{N\text{-}ter}$ (A. Kolodkin)(Terman et al., 2002), *UAS-GFP-2xFYVE* (M. Gonzalez-Gaitan)(Wucherpfennig et al., 2003), *ppk-Gal4* on II and III (Y. Jan) (Grueber et al., 2003), *SOP-flp (#42)* (a kind gift from T. Uemura), *UAS-Sec31-mCherry* (S. Luschnig)(Forster et al., 2010), *UAS-Sec15-GFP* (H. Bellen)(Jafar-Nejad et al., 2005), *UAS-Arf6*^{DN} (E. Chen), *UAS-Arf6* (E. Chen), *loner*^{T1032}(E. Olson)(Chen et al., 2003), *UAS-Step*^{DN} (T. Harris)(Lee and Harris, 2013), *Arl1*^{1} (J. Kennison)(Tamkun et al., 1991).

The following stocks were obtained from Bloomington Stock Center (BSC): *Gal4*$^{109(2)80}$, *elav-Gal4*, Control RNAi (BL#50613), *nrg* RNAi #1 (BL#38215), *nrg* RNAi #2 (BL#37496), *ppk-CD4-tdGFP* (BL#35843), *GSG2295-Gal4* (BL#40266), *Sec71* RNAi #1 (BL#32366), *UAS-GalT-GFP* (BL#30902), *UAS-Rab4-mRFP* (BL#8505), *UAS-mito-HA-GFP* (BL#8442).

The following Stocks were obtained from Vienna *Drosophila* RNAi Center (VDRC): *Sec71* RNAi #2 (v100300), *Arf1* RNAi #1 (v23082), *Arf1* RNAi #2 (v103572).

The following stocks were obtained from Kyoto Stock Center: *Sec71*^{GS16990} (#206863).

Generation of *Sec71* mutants

We crossed *Sec71*^{GS16990} flies with a fly strain carrying the Δ*2–3* transposase to induce imprecise excision. About 150 lines were established on the basis of the absence of the *w*+ marker. 56 lethal lines were isolated and subjected to genomic PCR and DNA sequencing analysis. The line with a 1461-bp deletion was named *Sec71*^{Ex11} (Figure S3A). The

Development • Supplementary information

Sec71^{GS16990} insertion line probably hopped from the original insertion site to the second intron and created this imprecise excision mutant.

Immunohistochemistry and antibodies

The following primary antibodies were used for immunohistochemistry at the indicated dilution: guinea pig anti-Avl (1:500; Yu Lab) (Zhang et al., 2014), rabbit anti-GM130 (1:200, Abcam ab52649), mouse anti-Ubiquitin (1:500; FK2, Enzo Life Sciences BML-PW0150-0100), mouse anti-Nrg (1:20, BP104, DSHB), rabbit anti-Lva antibody (1:1000, a gift from W. Sullivana)(Sisson et al., 2000), guinea pig anti-Arf1 (1:200, Yu Lab), mouse and guinea pig anti-Sec71 (1:200, Yu Lab), rabbit anti-GFP (1:1000, Invitrogen A11122), Cy3-, Cy5- or fluorescein isothiocyanate (FITC) conjugated secondary antibodies (Jackson Laboratories, Cat#: 111-165-003, 112-095-003, 111-175-003) were used at 1:400 dilution. For immunostaining, pupae or larvae were dissected in PBS and fixed with 4% formaldehyde for 20 min. Mounting was performed in VectaShield mounting medium, and the samples were directly visualized by confocal microscopy.

Generation of *Arf1, Sec71* and other transgenes

The *Arf1* and *Sec71* full-length cDNA were PCR from EST LD24904 and LD29171 (DGRC) into Topo Entry and pDonor, respectively (Life Tech). The dominant-negative variant of *Sec71* was generated by E677K site mutagenesis (Agilent Tech). The GDP-locked and GTP-locked constructs of *Arf1* were generated by T31N and Q71L site mutagenesis, respectively. Sec71 RNAi-resistant construct against Sec71 RNAi #1 was generated by site mutagenesis using following two primers CGTCATTTCGAATGGGTTTAAGTTCA ACGAGTCC and GGACTCGTTGAACTTAAAC CCATTCGAAATGACG.

The GATEWAY pTW vector containing the respective fragment of the cDNA were constructed by LR reaction (Life Tech) and several transgenic lines were established by the Bestgene Inc. An Arf1 RNAi-resistant cDNA was synthesized with a silent mutation on the

Development • Supplementary information

third base of each codon (First Base Tech), and was subjected to subcloning into pUAST and generation of transgenic lines. The *Sec71* variants were generated by site mutagenesis (Agilent Tech) and subcloned into pTWF-attB and targeted to the attP2 site.

The cDNA fragment encoding the aa 1-100 portion of rat ManII protein were amplified by PCR, subcloned into Topo entry and pTWV to generate ManII-Venus transgene (Bestgene Inc).

Arf1 and Sec71 antibody production

The cDNA fragment corresponding to the aa 60-345 fragment of Sec71 was amplified by PCR and verified by DNA sequencing. The product was expressed using the MBP expression vector (pMAL, NEB) and the purified protein was used to immunize guinea pigs and mice to generate antibodies against Sec71. The Arf1 full-length cDNA was amplified by PCR and verified by DNA sequencing. The product was expressed using the GST expression vector (pGEX 4T-1, Pharmacia) and the purified protein was used to immunize guinea pigs to generate antibodies against Arf1. The specificity of these antibodies was verified in respective RNAi and/or mutant ddaC neurons.

MARCM analysis of ddaC neurons

We carried out MARCM clonal analysis, dendrite imaging, and branch quantification as previously described (Kirilly et al., 2009). Briefly, ddaC or da clones were picked up and imaged at the WP stage according to their location and the dendritic arbor morphology. The same da neurons were examined for dendrite pruning defects at 16 h APF.

Co-Immunoprecipitation (Co-IP) and GST pull-down assay

We carried out S2 cell culture and Western blotting as described below. Myc-Sec71, Flag-Arf1^{WT}, Flag-Arf1^{T31N} and Flag-Arf1^{Q71L} expression vectors were generated by Gateway cloning and were transfected into S2 cells using Effectene Transfection Reagent (Qiagen). Transfected S2 cells were homogenized with the lysis buffer (25 mM Tris pH8/27.5 mM

Development • Supplementary information

NaCl/20 mM KCl/25 mM sucrose/1 mM DTT/10% (v/v) glycerol/0.5% Nonidet P40) with protease inhibitors (Complete, Boehringer; PMSF 10 µg/ml, Sodium orthovanadate 10 µg/ml). The supernatants were used for immunoprecipitation with anti-Myc (1:2,000, ab32, Abcam) overnight at 4°C, followed by incubation with protein A/G beads (Pierce Chemical Co.) for 2 h. Protein A/G beads were washed four times with cold PBS. Bound proteins were separated by SDS-PAGE and analysed by Western blotting with anti-Myc, anti-Flag HRP-conjugated antibody.

$Arf1^{WT}$, $Arf1^{T31N}$ and $Arf1^{Q71L}$ were inserted into (pGEX 4T-1, Pharmacia). The GST pull-down assays were carried out as previously described. Briefly, glutathione-sepharose 4B beads (GE Healthcare) bounded GST-Arf1 fusion protein were incubated for 3 h with Myc-Sec71protein extracts derived from S2 cell cultures, respectively. Bound beads were washed one time with the lysis buffer, two times with PBS and subjected to immunoblotting. γ–GTP (G0635, Sigma-Aldrich, 0.2mM) was pre-incubated with GST-Arf1 at room temperature for 30 min and also added into the lysis buffer. The blot bands were quantified in ImageJ software.

Trafficking Assay

eL3 staged larvae were fed with RU486 for 12 h. For immunostaining, larvae were dissected in PBS and fixed with 4% formaldehyde for 20 min. The fillets were incubated with rat monoclonal anti-CD8α (1:100, CALTAG Laboratories) in PBS and washed for three times with PBS in the detergent-free condition, which was followed by Cy3- secondary antibody incubation and wished for three times in the detergent-free condition. The intensity of immunofluorescence was measured in the same confocal setting for both mutant and control.

In vitro guanine nucleotide exchange assay

Development • Supplementary information

We carried out the in vitro guanine nucleotide exchange assays as previously described (Mahajan et al., 2013). GST fusion proteins for the Sec7 domain of Sec71 (aa554-790), its dominant negative form (E-K) and Sec7 domain of hBIG1 were expressed using the GST expression vector pGEB. 6xHis-tagged Arf1^{WT} and 6xHis-tagged Arl1^{WT} were expressed via the vector pET37b. The 6xHis-Arf1 fusion proteins were subjected to Tobacco Etch Virus protease cleavage to remove the N-terminal 6xHis-tag followed by gel filtration. All fusion proteins were dialyzed against HK buffer (50 mM HEPES pH 7.5, 120 mM KCl). The exchange assays were conducted in a black 96-well plate (Greiner Bio-One). Each reaction had 150 µl HKM buffer (HK buffer supplemented with 1 mM MgCl2 and 1 mM DTT) containing 1 µM Mant-GMPPNP, 1 µM 6xHis-Arf1^{WT}/6xHis-Arl1^{WT}, and 1 µM EDTA and 0.7 mM testing GST proteins (GST, GST-Sec71, GST-Sec71^{EK}, or GST-Sec7-hBIG1). The fluorescence was monitored by Tecan Infinite M200 pro at 25 °C with the excitation at 360 nm and emission at 440 nm. The fluorescence data were collected every 30 or 50 seconds depending on the total number of samples per plate. The exchange kinetic traces with significant spikes were rejected. Single exponential curve fitting were analyzed in OriginPro 8.5 (Origin Lab).

Quantification of immunolabeling

We quantified the immunolabeling intensities of Nrg at 6 h APF, as described previously (Zhang et al., 2014). Basically, soma/dendrite/axon contours were outlined on the individual fluorescent channel according to the GFP channel in ImageJ software. After subtracting the background (Rolling Ball Radius=50) on the entire image of that channel, we measured the mean grey value in the marked areas in ddaC or ddaE on the same images and calculated their ratios. The ratios were normalized to corresponding average control values and subjected to one-way ANOVA and Bonferroni tests for comparison between different conditions (*p<0.05, **p<0.01, ***p<0.001, n.s., not significant). Graphs display the average

Development • Supplementary information

values of ddaC/ddaE ratios and the standard error of means (S.E.M). The number of samples (n) in each group is shown on the bars.

Quantification of ddaC dendrites

Live confocal images of ddaC neurons expressing *UAS-mCD8-GFP* driven by *ppk-GAL4* were shown at WP and 16h APF. The average number of primary and secondary dendrites attached to soma was counted from wild type or mutant ddaC neurons. Primary dendrites are attached to the soma, while secondary dendrites are attached to the soma via their respective primary dendrites. The number of samples (n) in each group is shown on the bars. Statistical significance was determined using either two-tailed Student's T test (two samples) or one-way ANOVA and Bonferroni test (multiple samples) (*p<0.05, **p<0.01, ***p<0.001, n.s., not significant). Error represent S.E.M. Dorsal is up in all images.

Genotypes of fly strains

Figure 1: (B) *w*; ppk-Gal4, UAS-mCD8GFP / +; UAS-Dcr2 / UAS*-Control RNAi. (C) *w*; ppk-Gal4, UAS-mCD8GFP / +; UAS-Dcr2 / UAS-Arf1* RNAi #1. (D) *w*; ppk-Gal4, UAS-mCD8GFP, UAS-Dcr2 / +; UAS-Arf1* RNAi#1 / *UAS-Arf1(RNAi Resistant).* (E) *w*; ppk-Gal4 / UAS-Arf1^{T31N}; ppk-Gal4, UAS-mCD8GFP / +*. (F, G) *w*; UAS-Arf1^{T31N}/* GSG2295-*Gal4, ppk-tdGFP*. (H) *w*; UAS-Arf1^{Q71L} /* GSG2295-*Gal4, ppk-tdGFP*. (I) *w*; UAS-Arf1^{WT} /* GSG2295-*Gal4, ppk-tdGFP*.

Figure 2: (A-A") *w*; ppk-Gal4 / +; UAS-GalT-GFP / +*. (B-B") *w*; ppk-Gal4 / ppk-Gal4; ppk-Gal4, UAS-mCD8GFP / ppk-Gal4, UAS-mCD8GFP*. (C-C") *w*; ppk-Gal4 / +; UAS-Sec31-mCherry / +*. (D) *w*;* GSG2295-*Gal4 / UAS-Arf1^{T31N}; UAS-GalT-GFP / +*. (E) *w*; UAS-Arf1^{T31N}/* GSG2295-*Gal4, ppk-tdGFP* . (F) *w*;* GSG2295-*Gal4 / UAS-Arf1^{T31N}; UAS-Sec31-mCherry / +*. (G-G") *w*; ppk-Gal4, UAS-mCD8RFP, UAS-Dcr2 / +; UAS-ManII-Venus / +*. (H-H") *w*; ppk-Gal4, UAS-mCD8RFP, UAS-Dcr2 / +; UAS-ManII-Venus / UAS-Arf1* RNAi #1.

Figure 3: (A) *w*; ppk-Gal4, UAS-mCD8GFP / +; UAS-Dcr2 / UAS*-Control RNAi. (B) *w*; ppk-Gal4, UAS-mCD8GFP / +; UAS-Dcr2 / UAS-Sec71* RNAi #1. (C) *w*; ppk-Gal4, UAS-mCD8GFP, UAS-Dcr2 / +; UAS-Sec71(RNAi-Resistant) / UAS-Sec71* RNAi #1. (D) *w*; ppk-Gal4 / UAS-Sec71* RNAi #2*; ppk-Gal4, UAS-mCD8GFP / ppk-Gal4, UAS-mCD8GFP, UAS-Dcr2*. (E, F) *w*; UAS-Sec71^{DN} /* GSG2295-*Gal4, ppk-tdGFP* .

Development • Supplementary information

Figure 4: (G) *w*; ppk-Gal4, UAS-mCD8GFP, UAS-Dcr2 / +; UAS-Mical$^{N\text{-}ter}$ / UAS-Sec71* RNAi #1. (H) *w*; ppk-Gal4, UAS-mCD8GFP, UAS-Dcr2 / UAS-Arf1^{WT};UAS-Sec71* RNAi #1 / +.

Figure 5: (A-A") *w*; ppk-Gal4 / +; UAS-GalT-GFP / +*. (B-B") *w*; ppk-Gal4 / ppk-Gal4; ppk-Gal4, UAS-mCD8GFP / ppk-Gal4, UAS-mCD8GFP*. (C-C") *w*; ppk-Gal4 / ppk-Gal4; ppk-Gal4, UAS-mCD8GFP / ppk-Gal4, UAS-mCD8GFP*. (D-D") *w*; ppk-Gal4 / +; UAS-Sec31-mcherry / +*. (E) *w*;* GSG2295-*Gal4 / UAS-Sec71^{DN}; UAS-GalT-GFP / +*. (F) *w*; UAS-Sec71^{DN}* / GSG2295-*Gal4, ppk-tdGFP*. (G) *w*;* GSG2295-*Gal4 / UAS-Sec71^{DN}; UAS-Sec31-mcherry / +*. (H) *w*; ppk-Gal4 / ppk-Gal4; ppk-Gal4, UAS-mCD8GFP / ppk-Gal4, UAS-mCD8GFP*. (H') *w*; ppk-Gal4, UAS-mCD8GFP / +; UAS-Dcr2 / UAS-Sec71* RNAi #1. (H") *w*; UAS-Sec71^{DN}* / GSG2295-*Gal4, ppk-tdGFP* . (I) *w*; ppk-Gal4 / ppk-Gal4; ppk-Gal4, UAS-mCD8GFP / ppk-Gal4, UAS-mCD8GFP*. (I') *w*; ppk-Gal4, UAS-mCD8GFP / +; UAS-Dcr2 / UAS-Arf1* RNAi #1. (I") *w*; UAS-Arf1^{T31N}* / GSG2295-*Gal4, ppk-tdGFP* .

Figure 6: (B) *w*; ppk-Gal4, UAS-mCD8GFP, UAS-Dcr2; UAS-Mical$^{N\text{-}ter}$ / UAS-Sec71* RNAi #1. (C) *w*; ppk-Gal4, UAS-mCD8GFP, UAS-Dcr2 / +; UAS-Sec71 (RNAi-Resistant) / UAS-Sec71* RNAi #1. (D) *w*; ppk-Gal4, UAS-mCD8GFP, UAS-Dcr2 / +; UAS-Sec71$^{\Delta DCB}$ / UAS-Sec71* RNAi #1. (E) *w*; ppk-Gal4, UAS-mCD8GFP, UAS-Dcr2 / +; UAS-Sec71$^{\Delta HDS2\text{-}4}$ / UAS-Sec71* RNAi #1. (F) *w*; ppk-Gal4, UAS-mCD8GFP, UAS-Dcr2 / +; UAS-Sec71$^{\Delta HDS3\text{-}4}$ / UAS-Sec71* RNAi #1.

Figure 7: (A) *w*; ppk-Gal4 / ppk-Gal4; ppk-Gal4, UAS-mCD8GFP / ppk-Gal4, UAS-mCD8GFP*. (B) *w*; ppk-Gal4, UAS-Rab5^{DN} / +; ppk-Gal4, UAS-mCD8GFP / +*. (C) *w*; UAS-Arf1^{T31N}* / GSG2295-*Gal4, ppk-tdGFP*. (D) *w*; UAS-Sec71^{DN}* / GSG2295-*Gal4, ppk-tdGFP* . (F) *w*; ppk-Gal4, UAS-mCD8GFP, UAS-Dcr2 / +; UAS*-Control RNAi / *UAS-Arf1* RNAi #1. (G) *w*; ppk-Gal4, UAS-mCD8GFP, UAS-Dcr2 / UAS- nrg* RNAi *#1; UAS-Arf1* RNAi #1 / +. (H) *w*; ppk-Gal4, UAS-mCD8GFP, UAS-Dcr2 / UAS- nrg* RNAi *#2; UAS-Arf1* RNAi #1 / +. (J) *w*; ppk-Gal4, UAS-mCD8GFP, UAS-Dcr2 / +; UAS*-Control RNAi / *UAS-Sec71* RNAi #1. (K) *w*; ppk-Gal4, UAS-mCD8GFP, UAS-Dcr2 / UAS- nrg* RNAi *#1; UAS- Sec71* RNAi #1 / +. (L) *w*; ppk-Gal4, UAS-mCD8GFP, UAS-Dcr2 / UAS- nrg* RNAi *#2; UAS-Sec71* RNAi #1 / +.

Figure S1: (A) **Control:** *w*; ppk-Gal4, UAS-mCD8GFP / +; UAS-Dcr2 / UAS*-Control RNAi. ***Arf1* RNAi #2:** *w*; ppk-Gal4, UAS-mCD8GFP / UAS-Arf1* RNAi #2; *UAS-Dcr2 / +*. ***Arf1^{WT}*:** *w*; ppk-Gal4 / UAS-Arf1^{WT}; ppk-Gal4, UAS-mCD8GFP / +*. (B) **Wild type:** *w*; Gal4$^{109(2)80}$, UAS-mCD8GFP, SOP-flp / +; FRT82B / FRT82B, tubP-Gal80*. ***Arf1^{T31N}*:** *w*; Gal4$^{109(2)80}$, UAS-mCD8GFP, SOP-flp / UAS-Arf1^{DN}; FRT82B / FRT82B, tubP-Gal80*. **Wild type:** *w*;* GSG2295-*Gal4 / +; UAS-mCD8GFP / UAS-Mical$^{N\text{-}Ter}$*. ***Arf1^{T31N}*:** *w*;* GSG2295-*Gal4 / UAS-Arf1^{T31N}; UAS-mCD8GFP / +*. ***Arf1* RNAi #1:** *w*; ppk-Gal4, UAS-mCD8GFP / +; UAS-Dcr2 / UAS-Arf1* RNAi #1. (C) **Wild type:** *w*;; ppk-Gal4, UAS-mCD8GFP / ppk-Gal4, UAS-mCD8GFP*. ***Arf6^{DN}*:** *w*; ppk-Gal4 / UAS-Arf6^{DN}; ppk-Gal4, UAS-mCD8GFP / +*. ***Arl1^{1}:*** *w*; ppk-Gal4, UAS-mCD8GFP, SOP-flp #42/+; Arl1^{1},FRT2A/ tubP-Gal80,FRT2A*. (D) **Control RNAi:** *w*; ppk-Gal4, UAS-mCD8GFP / +; UAS-Dcr2 / UAS*-Control RNAi.

Development • Supplementary information

***Arf1* RNAi #1:** *w*; ppk-Gal4, UAS-mCD8GFP / +; UAS-Dcr2 / UAS-Arf1* RNAi #1. ***Sec71* RNAi #1:** *w*; ppk-Gal4, UAS-mCD8GFP / +; UAS-Dcr2 / UAS- Sec71* RNAi #1.

Figure S2: (A) **Wild type:** *w*; ppk-Gal4, UAS-mCD8GFP / ppk-Gal4, UAS-mCD8GFP; UAS-Dcr2 / UAS-Dcr2*. ***Arf1* RNAi #1**: *w*; ppk-Gal4, UAS-mCD8GFP / +; UAS-Dcr2 / UAS-Arf1* RNAi #1. ***Arf1* RNAi #2**: *w*; ppk-Gal4, UAS-mCD8GFP / UAS-Arf1* RNAi #2; *UAS-Dcr2 / +*. (B) *w*; ppk-Gal4 / ppk-Gal4; ppk-Gal4, UAS-mCD8GFP / ppk-Gal4, UAS-mCD8GFP*. (C) *w*; ppk-Gal4 / UAS-Rab4-mRFP*. (D) *w*; ppk-Gal4 / UAS-GFP-Rab5*. (E) *w*; ppk-Gal4 / UAS-mito-HA-GFP*. (F**) Wild type:** *w*; ppk-Gal4, UAS-mCD8RFP, UAS-Dcr2 / +; UAS-GalT-GFP / +*. ***Arf1* RNAi**: *ppk-Gal4, UAS-mCD8RFP, UAS-Dcr2 / +; UAS-GalT-GFP / UAS-Arf1* RNAi #1. ***Sec71* RNAi**: *ppk-Gal4, UAS-mCD8RFP, UAS-Dcr2 / +; UAS-GalT-GFP / UAS-Sec71*RNAi #1. (G) *w*; ppk-Gal4, UAS-mCD8RFP, UAS-Dcr2 / +; UAS-GalT-GFP / +*. (H) *w*; ppk-Gal4, UAS-mCD8RFP, UAS-Dcr2 / +; UAS-GalT-GFP / UAS-Arf1* RNAi #1.

Figure S3: (B) ***Sec71*^{Ex11}:** *w*; Sec71^{Ex11}, FRT40A / tubP-Gal80, FRT40A; ppk-Gal4, UAS-mCD8GFP, SOP-flp / +*. ***Sec71*^{Ex11} Rescue:** *elav-Gal4, UAS-mCD8GFP, hs-FLP, w* / Gal4$^{5-40}$, UAS-Venus:pm, SOP-flp #42 ; Sec71^{Ex11}, FRT40A / tubP-Gal80, FRT40A; UAS-Sec71^{FL} / +*. (C) **Wild type:** *w*; Gal4$^{109(2)80}$, UAS-mCD8GFP, SOP-flp / +; FRT82B / FRT82B, tubP-Gal80*. ***Sec71*^{DN}:** *w*; Gal4$^{109(2)80}$, UAS-mCD8GFP, SOP-flp / UAS-Sec71^{DN}; FRT82B / FRT82B, tubP-Gal80*. (D) **Wild type:** *w*;* GSG2295-*Gal4 / +; UAS-mCD8GFP / UAS-Mical^{N-Ter}*. ***Sec71*^{DN}:** *w*;* GSG2295-*Gal4 / UAS-Sec71^{DN}; UAS-mCD8GFP / +*. ***loner*^{T1032}:** *elav-Gal4, UAS-mCD8GFP, hs-FLP, w* / Gal4$^{5-40}$, UAS-Venus:pm, SOP-flp #42;; FRT82B, loner^{T1032} / FRT82B, tubP-Gal80*. ***Step*^{DN}:** *w*; ppk-Gal4 / +; ppk-Gal4, UAS-mCD8GFP / UAS-step^{DN}*. (E) **Control RNAi:** *w*; ppk-Gal4, UAS-mCD8GFP / +; UAS-Dcr2 / UAS-Control* RNAi. ***Sec71* RNAi #1:** *w*; ppk-Gal4, UAS-mCD8GFP / +; UAS-Dcr2 / UAS-Sec71* RNAi #1.

Figure S4: (C) ***Sec71* RNAi #1+UAS control:** *w*; ppk-Gal4, UAS-mCD8GFP, UAS-Dcr2 / +; UAS-Mical^{N-ter} / UAS-Sec71* RNAi #1. ***Sec71* RNAi #1 + *Arf6*^{WT}:** *w*; ppk-Gal4, UAS-mCD8GFP, UAS-Dcr2 / UAS-Arf6^{WT};UAS-Sec71* RNAi #1 / +.

Figure S5: (A)**Wild type:** *w*; ppk-Gal4, UAS-mCD8GFP / ppk-Gal4, UAS-mCD8GFP; UAS-Dcr2 / UAS-Dcr2*. ***Sec71* RNAi #1**: *w*; ppk-Gal4, UAS-mCD8GFP / +; UAS-Dcr2 / UAS-Sec71* RNAi #1. ***Sec71*^{Ex11}:** *w*; Sec71^{Ex11}, FRT40A / tubP-Gal80, FRT40A; ppk-Gal4, UAS-mCD8GFP, SOP-flp / +*. (B) **Wild type**: *w*; ppk-Gal4 / UAS-Sec15-GFP*. (C) **Wild type**: *w*; ppk-Gal4, UAS-Dcr2 / UAS-Sec15-GFP*. ***Arf1* RNAi:** *w*; ppk-Gal4, UAS-Dcr2 / UAS-Sec15-GFP; UAS-Arf1* RNAi #1 / +. ***Sec71* RNAi:** *w*; ppk-Gal4 / UAS-Sec15-GFP; UAS-Sec71* RNAi #1 / +. (D) **Wild type:** *w*;* GSG2295-*Gal4 / +; UAS-mCD8GFP / UAS-Mical^{N-Ter}*. ***Arf1*^{T31N}:** *w*;* GSG2295-*Gal4 / UAS-Arf1^{T31N}; UAS-mCD8GFP / +*. ***Sec71*^{DN}:** *w*;* GSG2295-*Gal4 / UAS-Sec71^{DN}; UAS-mCD8GFP / +*.

Figure S6: (B) ***Sec71*^{FL}:** *w*; ppk-Gal4 / +; UAS-GalT-GFP / UAS-Sec71* (RNAi-Resistant). ***Sec71*$^{\Delta DCB}$:** *w*; ppk-Gal4 / +; UAS-GalT-GFP / UAS-Sec71$^{\Delta DCB}$*. ***Sec71*$^{\Delta HUS}$:** *w*; ppk-Gal4 /*

Development • Supplementary information

+; UAS-GalT-GFP / UAS-Sec71$^{\Delta HUS}$. ***Sec71$^{\Delta HDS1}$:*** *w*; ppk-Gal4 / +; UAS-GalT-GFP / UAS-Sec71$^{\Delta HDS1}$.* ***Sec71$^{\Delta HDS2-4}$:*** *w*; ppk-Gal4 / +; UAS-GalT-GFP / UAS-Sec71$^{\Delta HDS2-4}$.* ***Sec71$^{\Delta HDS3-4}$:*** *w*; ppk-Gal4 / +; UAS-GalT-GFP / UAS-Sec71$^{\Delta HDS3-4}$.*

Figure S7: (A) **Wild type:** *w*;* GSG2295-*Gal4 / +; UAS-GFP-2×FYVE / UAS-Mical^{N-Ter}.* ***Arf1^{T31N}:*** *w*;* GSG2295-*Gal4 / UAS-Arf1^{T31N}; UAS-GFP-2×FYVE / +.* ***Sec71^{DN}:*** *w*;* GSG2295-*Gal4 / UAS-Sec71^{DN}; UAS-GFP-2×FYVE / +.* (B-C) ***Rab5^{DN}:*** *w*; UAS-Rab5^{DN} /* GSG2295-*Gal4; ppk-tdGFP / UAS-Mical^{N-Ter}.* ***Arf1^{T31N}:*** *w*; UAS-Arf1^{T31N} /* GSG2295-*Gal4; ppk-tdGFP / UAS-Mical^{N-Ter}.* ***Rab5^{DN}; Arf1^{T31N}:*** *w*; UAS-Arf1^{T31N} /* GSG2295-*Gal4, UAS-Rab5^{DN}; ppk-tdGFP / +.* ***Sec71^{DN}:*** *w*; UAS-Sec71^{DN} /* GSG2295-*Gal4; ppk-tdGFP / UAS-Mical^{N-Ter}.* ***Rab5^{DN}; Sec71^{DN}:*** *w*; UAS-Sec71^{DN} /* GSG2295-*Gal4, UAS-Rab5^{DN}; ppk-tdGFP / +.*

Supplemental References

Chen, E. H., Pryce, B. A., Tzeng, J. A., Gonzalez, G. A. and Olson, E. N. (2003). Control of myoblast fusion by a guanine nucleotide exchange factor, loner, and its effector ARF6. ***Cell*** **114, 751-62.**

Forster, D., Armbruster, K. and Luschnig, S. (2010). Sec24-dependent secretion drives cell-autonomous expansion of tracheal tubes in Drosophila. ***Curr Biol*** **20, 62-8.**

Grueber, W. B., Jan, L. Y. and Jan, Y. N. (2003). Different levels of the homeodomain protein cut regulate distinct dendrite branching patterns of Drosophila multidendritic neurons. ***Cell*** **112, 805-18.**

Jafar-Nejad, H., Andrews, H. K., Acar, M., Bayat, V., Wirtz-Peitz, F., Mehta, S. Q., Knoblich, J. A. and Bellen, H. J. (2005). Sec15, a component of the exocyst, promotes notch signaling during the asymmetric division of Drosophila sensory organ precursors. ***Dev Cell*** **9, 351-63.**

Kirilly, D., Gu, Y., Huang, Y., Wu, Z., Bashirullah, A., Low, B. C., Kolodkin, A. L., Wang, H. and Yu, F. (2009). A genetic pathway composed of Sox14 and Mical governs severing of dendrites during pruning. ***Nat Neurosci*** **12, 1497-505.**

Lee, D. M. and Harris, T. J. (2013). An Arf-GEF regulates antagonism between endocytosis and the cytoskeleton for Drosophila blastoderm development. ***Curr Biol*** **23, 2110-20.**

Mahajan, D., Boh, B. K., Zhou, Y., Chen, L., Cornvik, T. C., Hong, W. and Lu, L. (2013). Mammalian Mon2/Ysl2 regulates endosome-to-Golgi trafficking but possesses no guanine nucleotide exchange activity toward Arl1 GTPase. ***Sci Rep*** **3, 3362.**

Sisson, J. C., Field, C., Ventura, R., Royou, A. and Sullivan, W. (2000). Lava lamp, a novel peripheral golgi protein, is required for Drosophila melanogaster cellularization. ***J Cell Biol*** **151, 905-18.**

Tamkun, J. W., Kahn, R. A., Kissinger, M., Brizuela, B. J., Rulka, C., Scott, M. P. and Kennison, J. A. (1991). The arflike gene encodes an essential GTP-binding protein in Drosophila. ***Proc Natl Acad Sci U S A*** **88, 3120-4.**

Terman, J. R., Mao, T., Pasterkamp, R. J., Yu, H. H. and Kolodkin, A. L. (2002). MICALs, a family of conserved flavoprotein oxidoreductases, function in plexin-mediated axonal repulsion. ***Cell*** **109, 887-900.**

Wucherpfennig, T., Wilsch-Brauninger, M. and Gonzalez-Gaitan, M. (2003). Role of Drosophila Rab5 during endosomal trafficking at the synapse and evoked neurotransmitter release. ***J Cell Biol*** **161, 609-24.**

Zhang, H., Wang, Y., Wong, J. J., Lim, K. L., Liou, Y. C., Wang, H. and Yu, F. (2014). Endocytic pathways downregulate the L1-type cell adhesion molecule neuroglian to promote dendrite pruning in Drosophila. ***Dev Cell*** **30, 463-78.**

Development • Supplementary information